Electronic supporting information for

Multichromophoric *COO*-BODIPYs: An advantageous design for the development of energy transfer and electron transfer systems

César Ray,[a] Christopher Schad,[a] Edurne Avellanal-Zaballa,[b] Florencio Moreno,[a] Beatriz L. Maroto,[a] Jorge Bañuelos,*[b] Inmaculada García-Moreno,[c] and Santiago de la Moya*[a]

[a] *Depto. de Química Orgánica I, Facultad de CC. Químicas, Universidad Complutense de Madrid, Ciudad Universitaria s/n, 28040, Madrid, Spain. E-mail: santmoya@ucm.es*

[b] *Depto. de Química Física, Universidad del Pais Vasco-EHU, Apartado 644, 48080, Bilbao, Spain. E-mail: jorge.banuelos@ehu.es*

[c] *Depto. de Sistemas de Baja Dimensionalidad, Superficies y Materia Condensada, Instituto de Química-Física Rocasolano, Centro Superior de Investigaciones Científicas (CSIC), Serrano 119, 28006 Madrid, Spain.*

Table of contents

1. General methods, instrumentation and techniques

Synthesis

All reagents were used without purification. All solvents were of HPLC grade and were dried according to standard methods. Starting chemical substrates and reagents were used as commercially provided unless otherwise indicated. Thin-layer chromatography (TLC) was performed on silica gel and the chromatograms were visualized using UV light (λ = 254 or 365 nm). Flash column chromatography was performed using silica gel (230-400 mesh). ^{1}H, ^{13}C, ^{11}B and ^{19}F NMR spectra were recorded in $CDCl_3$ or THF-d_8 solution at 20 ºC. NMR chemical shifts are expressed in parts per million (δ scale). ^{1}H and ^{13}C NMR spectra are referenced to residual protons of $CDCl_3$ (δ = 7.26 and 77.16 ppm, respectively) or TFH-d_8 (δ = 1.73 and 35.37 ppm, respectively) as internal standard, ^{11}B and ^{19}F NMR spectra are referenced to 15% $BF_3{\cdot}Et_2O$ in $CDCl_3$ (δ = 0.00 ppm) and trifluorotoluene (δ = -63.72 ppm) as external standard, respectively. The type of carbon (C, CH, CH_2 or CH_3) was assigned by DEPT-135 NMR experiments. Additionally, complex spin-system signals were simulated by using MestReNova program version 10.0.1-14719. FTIR spectra were obtained from neat samples using the attenuated total reflection (ATR) technique. High-resolution mass spectrometry (HRMS) was performed by using direct sample injection, electrospray ionization (ESI) and hybrid quadrupole time-of-flight mass analyser (QTOF; positive- or negative-ion mode are indicated as ESI^+ and ESI^-, respectively).

Photophysics

Photophysical signatures were recorded using quartz cuvettes of 1 cm optical path-length and diluted dye solutions (*ca.* $2{\cdot}10^{-6}$ M) prepared from a concentrated stock solution in chloroform (*ca.* 10^{-3} M), after solvent evaporation under reduced pressure, and subsequent dilution with the desired solvent of spectroscopic grade. UV-vis absorption and fluorescence spectra were recorded on a Varian (model CARY 4E) spectrophotometer and an Edinburgh Instrument spectrofluorimeter (model FLSP 920), respectively. Concentrated dye solutions (mM) were measured using quartz cuvettes with an optical path-length of 0.01 mm and front-face configuration in the fluorescence spectra to avoid reabsorption and reemission phenomena.

Fluorescence quantum yields (ϕ_{fl}) were determined from corrected spectra (detector sensibility to the wavelength) by the optically dilute relative method and by using Eq. 1, where I_{exc} is the luminescent intensity at the excitation wavelength, A_{exc} is the absorbance at the excitation wavelength, $\int I d\lambda$ is the numerically integrated intensity from the luminescence spectra, and n is the index of refraction of the solution. The subscripts *R* and *S* denote reference and sample, respectively. PM567 in acetone (ϕ_f = 0.85)[1] was used as the reference.

$$\phi_S/\phi_R = (\int I_S d\lambda / \int I_R d\lambda)\,(I_{R,exc} / I_{S,exc})\,(A_{R,exc} / A_{S,exc})\,(n_S / n_R)^2 \qquad \text{Eq. 1}$$

The aforementioned spectrofluorimeter is also equipped with a wavelength-tunable pulsed Fianium laser. Thus, the Time Correlated Single-Photon Counting (TCSPC) technique was used to record the fluorescence decay curves. Fluorescence emission was monitored at the maximum emission wavelength after excitation by the said Fianium at the maximum absorption wavelength. The fluorescence lifetime (τ) was obtained from the slope of the exponential fit of the decay curve, after the deconvolution of the instrumental response signal (recorded by means of a ludox scattering suspension) by means of an iterative method. The goodness of the exponential fit was controlled by statistical parameters (chi-square, Durbin-Watson and the analysis of the residuals).

Excitation energy transfer efficiency, *EETE*, was determined by measuring the quenching of the donor fluorescence caused by the energy transfer to the acceptor by using Eq. 2; where ϕ_D is the fluorescence quantum yield of the energy donor covalently linked to the energy acceptor, and ϕ_D^0 is the corresponding value for the free donor.

$$EETE = (1- \phi_D/\phi_D^0)\cdot 100 \qquad \text{Eq. 2}$$

Computational chemistry

Ground state geometries were optimized with the range-separated wb97xd hybrid functional, within the Density Functional Theory (DFT), using the triple valence basis set with a polarization function (6-311G*). The geometries were considered as energy minimum when the corresponding frequency analysis did not give any negative value. The absorption spectra were predicted as vertical Franck-Condon transitions from the optimized ground state geometries using the Time Dependent (td) method with the aforementioned DFT functional and basis set. The solvent effect (cyclohexane) was taking into account during the energy minimization and energetic arrangement of the molecular orbitals by means of the Polarizable Continuum Model (PCM). All the theoretical calculations were carried out using the GAUSSIAN 16 program suite, implemented in the computational cluster provided by the SGIker resources of UPV-EHU.

Lasing

Laser efficiency was evaluated from concentrated solutions (milimolar) of dyes in ethyl acetate contained in 1-cm optical-path rectangular quartz cells carefully sealed to avoid solvent evaporation during experiments. The liquid solutions were transversely pumped with 5 mJ, 8 ns FWHM pulses from the second harmonic (532 nm) and the third harmonic (355 nm) of a Q-switched Nd:YAG laser (Lotis TII 2134) at a repetition rate of 1 Hz. The exciting pulses were line-focused onto the cell using a combination of positive and negative cylindrical lenses (f = 15 cm and f = -15 cm, respectively) perpendicularly arranged. The plane parallel oscillation cavity (2-cm length) consisted of a 90% reflectivity aluminum mirror acting as back reflector, and the lateral face of the cell acting as output coupler (4% reflectivity). The pump and output energies were detected by a GenTec powermeter. The

photostability of the dyes was evaluated by using a pumping energy and geometry exactly equal to that of the laser experiments at 532 nm. We used spectroscopic quartz cuvettes with 0.1-cm optical path to allow for the minimum solution volume (40 μL) to be excited. The lateral faces were ground, whereupon no laser oscillation was obtained. Information about photostabilitiy was obtained by monitoring the decrease in laser-induced fluorescence (LIF) intensity after 20000 pump pulses and 15 Hz repetition rate to speed up the experimental running. The fluorescence emission and laser spectra were monitored perpendicular to the exciting beam, collected by an optical fiber, and imaged onto a spectrometer (Acton Research corporation) and detected with a charge-coupled device (CCD) (SpectruMM:GS128B). The fluorescence emission was recorded by feeding the signal to the boxcar (Stanford Research, model 250) to be integrated before being digitized and processed by a computer. The estimated error in the energy and photostability measurements was 10%.

2. Synthetic procedures and characterization data

At-boron functionalization: General procedure

BCl_3 (1 M in CH_2Cl_2; 0.32 mmol, 2 mol equiv.) was dropwise added over a solution of the corresponding *F*-BODIPY (0.16 mmol, 1 mol equiv.) in dry CH_2Cl_2 (5 mL) under Ar atmosphere. The reaction mixture was stirred at room temperature for 5 min. Then, triethylamine (0.96 mmol, 6 mol equiv.) was added, followed by addition of the *O*-nucleophile (2-naphthol or the corresponding carboxylic acid; 0.64 mmol, 4 mol equiv.) and the resulting mixture stirred for 30 min. Then, the reaction mixture was filtered through Celite® S, washing thoroughly with CH_2Cl_2 and the solvent evaporated under reduced pressure. The obtained residue was purified by flash chromatography to afford the desired MMA. See Scheme S1.

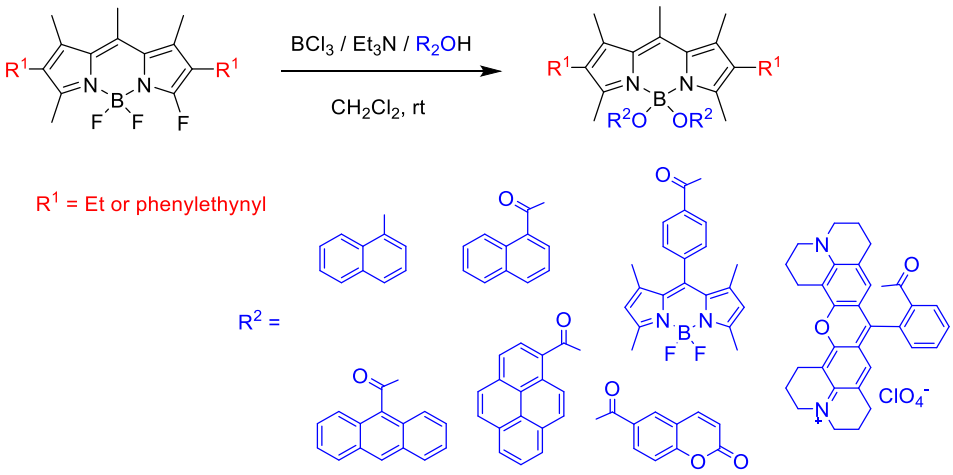

Scheme S1. General synthetic outline.

Synthesis of 3

According to the described general procedure, commercial PM567 (2,6-diethyl-4,4-difluoro-1,3,5,7,8-pentamethylBODIPY, 50 mg, 0.16 mmol) was reacted with 1-naphthol (90 mg, 0.62 mmol). The reaction crude was purified by flash chromatography (silica gel, hexane/CH_2Cl_2 1:1) to obtain **3** (71 mg, 80%) as an orange brown solid. R_F = 0.46 (hexane / CH_2Cl_2 1:1). ^{1}H NMR (THF-d_8, 300 MHz) δ 8.75 (d, *J* = 8.3 Hz, 2H), 7.66 (d, *J* = 8.3 Hz, 2H), 7.46 (ddd, *J* = 8.3, 6.8, 1.5 Hz, 2H), 7.38 (ddd, *J* = 8.1, 6.8, 1.4 Hz, 2H), 7.12 (d, *J* = 8.2 Hz, 2H), 6.92 (t, *J* = 8.0 Hz, 2H), 6.10 (dd, *J* = 7.8, 0.8 Hz, 2H), 2.92 (s, 3H), 2.47 (s, 6H), 2.28 (s, 6H), 2.22 (q, *J* = 7.6 Hz, 4H), 0.80 (t, *J* = 7.5 Hz, 6H) ppm. ^{13}C NMR (THF-d_8, 75 MHz) δ 153.9 (C), 153.7 (C), 141.0 (C), 137.5 (C), 136.1 (C), 133.7 (C), 133.6 (C), 129.2 (C), 128.0 (CH), 127.1 (CH), 126.3 (CH), 125.0 (CH), 124.2 (CH), 118.8 (CH), 109.5 (CH), 17.7 (CH_2), 17.4 (CH_3), 15.1 (CH_3), 14.7 (CH_3), 12.8 (CH_3) ppm. ^{11}B NMR (THF-d_8, 160 MHz) δ 1.11 ppm. HRMS (ESI$^-$) *m/z*: $[M - H]^-$ Calcd. for $C_{38}H_{38}BN_2O_2$ 565.3026; Found 565.3021.

Synthesis of 4a

According to the described general procedure, PM567 (50 mg, 0.16 mmol) was reacted with naphthalene-1-carboxylic acid (108 mg, 0.63 mmol). The reaction crude was purified by flash chromatography (silica gel, CH_2Cl_2) to obtain **4a** (86 mg, 88%) as an orange brown solid. R_F = 0.31 (hexane/ CH_2Cl_2 2:8). ^{1}H NMR ($CDCl_3$, 300 MHz) δ 9.09 (dm, J = 8.9 Hz, 2H), 8.46 (dd, J = 7.3, 1.3 Hz, 2H), 8.00 (d, J = 8.2 Hz, 2H), 7.91-7.83 (m, 2H), 7.58-7.45 (m, 6H), 2.80 (s, 3H), 2.45 (s, 6H), 2.42 (s, 6H), 2.33 (q, J = 7.6 Hz, 4H), 0.98 (t, J = 7.5 Hz, 6H) ppm. ^{13}C NMR ($CDCl_3$, 75 MHz) δ 167.0 (C), 150.1 (C), 140.8 (C), 136.8 (C), 134.1 (C), 133.4 (C), 132.7 (CH), 132.3 (C), 131.9 (C), 130.5 (CH), 129.6 (C), 128.5 (CH), 127.4 (CH), 126.7 (CH), 125.9 (CH), 124.8 (CH), 17.7 (CH_3), 17.4 (CH_2), 15.0 (CH_3), 14.96 (CH_3), 13.0 (CH_3) ppm. ^{11}B NMR ($CDCl_3$, 160 MHz) δ 0.53 ppm. FTIR ν 1701, 1557, 1202 cm^{-1}. HRMS (ESI$^+$) *m/z* [M + Na]$^+$ Calcd. for $C_{40}H_{39}BN_2NaO_4$ 645.2901, Found 645.2912.

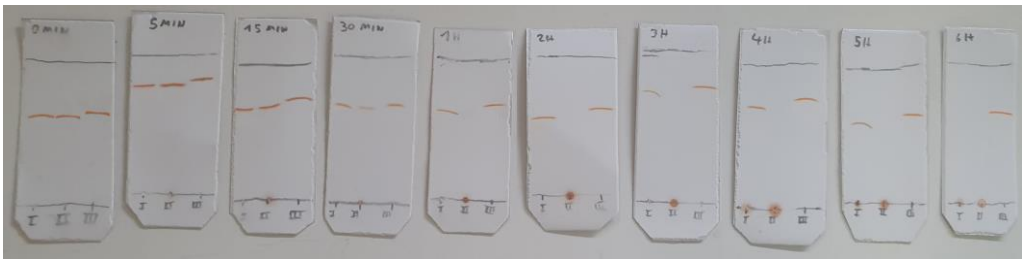

Fig. S1. Differential stability of *COO*-BODIPY **4a** (I), related *O*-BODIPY **3** (II) and parent *F*-BODIPY PM567 (III) towards harsh acidic conditions. Experimental details: 3 mL of an ethyl acetate solution of the corresponding dye (*ca.* 1·10^{-3} M) was stirred vigorously with 3 mL HCl 1 M at room temperature, and the evolution of the integrity of the dyes analyzed by TLC (silica gel; hexane/dichloromethane 2:3). The *F*-BODIPY (III) remains unaltered after 6-h treatment, whereas the *O*-BODIPY (II) and the corresponding *COO*-BODIPY (I) decompose completely after *ca.* 1-h treatment and *ca.* 6-h treatment, respectively. These results confirm the expected stability trend towards severe acidic conditions: *F*-BODIPY > *COO*-BODIPY > *O*-BODIPY.

Synthesis of 4b

According to the described general procedure, PM567 (50 mg, 0.16 mmol) was reacted with anthracene-9-carboxylic acid (140 mg, 0.63 mmol). The reaction crude was purified by flash chromatography (silica gel, CH_2Cl_2 / MeOH 95.5:0.5) to obtain **4b** (94 mg, 83%) as an orange solid. R_F = 0.26 (CH_2Cl_2). ^{1}H NMR ($CDCl_3$, 300 MHz) δ 8.35 (s, 2H), 7.90 (d, J = 8.2 Hz, 4H), 7.79 (d, J = 8.3 Hz, 4H), 7.37 (ddd, J = 8.1, 6.7, 1.3 Hz4H), 7.30 (ddd, J = 8.4, 6.7, 1.4 Hz, 4H), 2.58 (s, 6H), 2.57 (s, 3H), 2.44 (q, J = 7.6 Hz, 4H), 2.35 (s, 6H), 1.18 (t, J = 7.6 Hz, 6H) ppm. ^{13}C NMR ($CDCl_3$, 75 MHz) δ 170.0 (C), 150.1 (C), 140.7 (C), 137.2 (C), 133.3 (C), 132.9 (C), 131.7 (C), 131.1 (C), 128.3 (CH), 127.7 (CH), 127.5 (C), 125.84 (CH), 125.8 (CH), 125.2 (CH), 17.5 (CH_2), 17.4 (CH_3), 15.1 (CH_3), 14.8 (CH_3), 14.3 (CH_3) ppm. ^{11}B NMR ($CDCl_3$, 160 MHz) δ 0.52 ppm. FTIR ν 1692, 1554, 1205 cm^{-1}. HRMS (ESI$^+$) *m/z* [M + Na]$^+$ Calcd. for $C_{48}H_{43}BN_2NaO_4$ 745.3214, Found 745.3224.

Synthesis of 4c

According to the described general procedure, PM567 (50 mg, 0.16 mmol) was reacted with pyrene-1-carboxylic acid (155 mg, 0.63 mmol). The reaction crude was purified by flash chromatography (silica gel, CH_2Cl_2) to obtain **4c** (118 mg, 97%) as a red solid. R_F = 0.28 (hexane / CH_2Cl_2 2:8).^{1}H NMR ($CDCl_3$, 300 MHz) δ 9.46 (d, *J* = 9.5 Hz, 2H), 8.95 (d, *J* = 8.1 Hz, 2H), 8.28-8.22 (m, 6H), 8.20-8.10 (m, 6H), 8.05 (t, *J* = 7.6 Hz, 2H), 2.80 (s, 3H), 2.55 (s, 6H), 2.44 (s, 6H), 2.35 (q, *J* = 7.5 Hz, 4H), 1.00 (t, *J* = 7.5 Hz, 6H) ppm. ^{1}H NMR ($CDCl_3$, 500 MHz) δ 9.46 (d, *J* = 9.4 Hz, 2H), 8.95 (d, *J* = 8.1 Hz, 2H), 8.26 (d, *J* = 8.0 Hz, 2H), 8.25 (d, *J* = 7.6 Hz, 2H), 8.24 (d, *J* = 7.5 Hz, 2H), 8.18 (d, *J* = 9.1 Hz, 4H), 8.12 (d, *J* = 8.9 Hz, 2H), 8.05 (t, *J* = 7.6 Hz, 2H), 2.80 (s, 3H), 2.55 (s, 6H), 2.44 (s, 6H), 2.35 (q, *J* = 7.5 Hz, 4H), 1.00 (t, *J* = 7.5 Hz, 6H) ppm. ^{13}C NMR ($CDCl_3$, 75 MHz) δ 167.6 (C), 150.2 (C), 140.9 (C), 136.9 (C), 134.0 (C), 133.5 (C), 132.5 (C), 131.25 (C), 131.23 (C), 130.6 (C), 129.3 (CH), 129.1 (CH), 129.0 (CH), 127.4 (CH), 126.6 (C), 126.3 (CH), 126.1 (CH), 125.9 (CH), 125.9 (CH), 125.1 (C), 124.6 (C), 124.4 (CH), 17.7 (CH_3), 17.4 (CH_2), 15.02 (CH_3), 14.98 (CH_3), 13.1 (CH_3) ppm. ^{11}B NMR ($CDCl_3$, 160 MHz) δ 0.74 ppm. FTIR ν 1696, 1555, 1264, 1203 cm^{-1}. HRMS (ESI$^+$) *m/z* [M + Na]$^+$ Calcd. for $C_{52}H_{43}BN_2NaO_4$ 793.3214, Found 793.3229. HRMS (ESI$^-$) *m/z* [M - H]$^-$ Calcd. for $C_{52}H_{42}BN_2O_4$ 769.3238; Found 769.3261.

***Synthesis of* 4d**

According to the described general procedure, PM567 (50 mg, 0.16 mmol) was reacted with 6-carboxycoumarin (120 mg, 0.63 mmol). The reaction crude was purified by flash chromatography (silica gel, CH_2Cl_2) to obtain **4d** (93 mg, 86%) as an orange solid. R_F = 0.38 (CH_2Cl_2 / MeOH 9:1).^{1}H NMR ($CDCl_3$, 300 MHz) δ 8.34 (dd, *J* = 8.6, 2.0 Hz, 2H), 8.26 (d, *J* = 2 Hz, 2H), 7.77 (d, *J* = 9.6 Hz, 2H), 7.40 (d, *J* = 8.6 Hz, 2H), 6.47 (s, 9.6 Hz, 2H), 2.78 (s, 3H), 2.40 (s, 6H), 2.33 (s, 6H), 2.30 (q, *J* = 7.6 Hz, 4H), 0.95 (t, *J* = 7.5 Hz, 6H) ppm. ^{13}C NMR ($CDCl_3$, 75 MHz) δ 164.7 (C), 160.2 (C), 156.7 (C), 149.9 (C), 143.5 (CH), 141.0 (C), 137.2 (C), 133.3 (C), 133.2 (CH), 132.5 (C), 130.1 (CH), 129.1 (C), 118.6 (C), 117.3 (CH), 117.0 (CH), 17.5 (CH_3), 17.4 (CH_2), 14.95 (CH_3), 14.87 (CH_3), 12.7 (CH_3) ppm. ^{11}B NMR ($CDCl_3$, 160 MHz) δ 0.50 ppm. FTIR ν 1736, 1707, 1625, 1555, 1205 cm^{-1}. HRMS (ESI$^+$) *m/z* [M + Na]$^+$ Calcd. for $C_{38}H_{35}BN_2NaO_8$ 681.2384, Found 681.2389.

Synthesis of 4f

According to the described general procedure, PM567 (27 mg, 0.08 mmol) was reacted with rhodamine 640 perchlorate (200 mg, 0.34 mmol). The reaction crude was purified by flash chromatography (silica gel, CH_2Cl_2 / MeOH 97:3) to obtain **4f** (80 mg, 65%) as an purple solid. R_F = 0.34 (CH_2Cl_2 / MeOH 97:3). ^{1}H NMR ($CDCl_3$, 300 MHz) δ 8.15-8.07 (m, 2H), 7.78-7.67 (m, 4H), 7.11-7.03 (m, 2H), 6.47 (s, 4H), 3.60-3.40 (m, 16H), 3.08-2.89 (m, 8H), 2.72-2.49 (m, 8H), 2.32 (s, 3H), 2.14 (q, *J* = 7.4 Hz, 4H), 2.10 (s, 6H), 2.06-1.88 (m, 16H), 1.82 (s, 6H), 0.70 (t, *J* = 7.5 Hz, 6H) ppm.^{13}C NMR ($CDCl_3$, 75 MHz)

δ 163.9 (C), 157.3 (C), 152.2 (C), 151.1 (C), 149.5 (C), 140.6 (C), 136.6 (C), 134.0 (C), 132.9 (C), 132.7 (C), 132.3 (CH), 132.1 (C), 131.5 (CH), 130.9 (CH), 130.0 (CH), 126.6 (CH), 123.5 (C), 113.1 (C), 105.2 (C), 51.0 (CH_2), 50.5 (CH_2), 27.8 (CH_2), 20.8 (CH_2), 20.1 (CH_2), 19.8 (CH_2), 17.5 (CH_3), 17.1 (CH_2), 14.9 (CH_3), 14.6 (CH_3), 12.1 (CH_3) ppm.^{11}B NMR ($CDCl_3$, 160 MHz) δ -0.08 ppm. FTIR ν 1713, 1463, 1300 cm^{-1}. HRMS (ESI$^+$) *m/z*: $[M]^{2+}$ Calcd. for $C_{82}H_{85}BN_6O_6$ 630.3312; Found 630.3318. HRMS (ESI$^-$) *m/z*: $[M]^-$ Calcd. for ClO_4 98.9485, Found 98.9484.

Synthesis of 5c

According to the described general procedure, 2,6-bis(phenylethynyl)-4,4-difluoro-1,3,5,7,8-pentamethylBODIPY[2] (25 mg, 0.05 mmol) was reacted with pyrene-1-carboxylic acid (53 mg, 0.22 mmol). The reaction crude was purified by flash chromatography (silica gel, hexane / CH_2Cl_2 1:1) to obtain **5c** (45 mg, 91%) as a red solid. R_F = 0.29 (hexane / CH_2Cl_2 4:6). ^{1}H NMR ($CDCl_3$, 300 MHz) δ 9.54 (d, J = 9.5 Hz, 2H), 9.04 (d, J = 8.1 Hz, 2H), 8.32-8.17 (m, 10H), 8.14 (d, J = 8.9 Hz, 2H), 8.06 (t, J = 7.6 Hz, 2H), 7.46-7.37 (m, 4H), 7.28-7.21 (m, 6H), 2.94 (s, 3H), 2.77 (s, 6H), 2.71 (s, 6H) ppm. ^{13}C NMR ($CDCl_3$, 75 MHz) δ 167.5 (C), 155.2 (C), 143.7 (C), 142.3 (C), 134.4 (C), 133.9 (C), 131.7 (C), 131.4 (CH), 131.2 (C), 130.6 (C), 129.6 (CH), 129.4 (CH), 129.3 (CH), 128.4 (CH), 128.1 (CH), 127.4 (CH), 126.3 (CH), 126.2 (CH), 126.1 (CH), 125.7 (CH), 125.4 (C), 125.2 (C), 124.5 (C), 124.4 (CH), 123.6 (C), 116.3 (C), 96.4 (C), 82.1 (C), 17.8 (CH_3), 16.7 (CH_3), 14.4 (CH_3) ppm. ^{11}B NMR ($CDCl_3$, 160 MHz) δ 0.57 ppm. FTIR ν 1695, 1546, 1261, 1197, 1004 cm^{-1}. HRMS (ESI$^-$) *m/z* $[M - H]^-$ Calcd. for $C_{64}H_{42}BN_2O_4$ 913.3238, Found 937.3239.

Synthesis of 5e

According to the described general procedure, 2,6-bis(2-phenylethynyl)-4,4-difluoro-1,3,5,7,8-pentamethylBODIPY[2] (20 mg, 0.04 mmol) was reacted with 8-(4-carboxyphenyl)-1,3,5,7-tetramethylBODIPY[3] (63 mg, 0.17 mmol). The reaction crude was purified by flash chromatography (silica gel, hexane / AcOEt 8:2) to obtain **5e** (33 mg, 66%) as a reddish violet solid. R_F = 0.30 (CH_2Cl_2). ^{1}H NMR ($CDCl_3$, 700 MHz) δ 8.28 (d, J = 8.3 Hz, 4H), 7.47-7.44 (m, 4H), 7.40 (d, J = 8.4 Hz, 4H), 7.34-7.30 (m, 6H), 5.98 (s, 4H), 2.90 (s, 3H), 2.67 (s, 6H), 2.60 (s, 6H), 2.56 (s, 12H), 1.37 (s, 12H) ppm. ^{13}C NMR ($CDCl_3$, 176 MHz) δ 165.7 (C), 156.1 (C), 154.9 (C), 143.8 (C), 143.1 (C), 142.5 (C), 140.6 (C), 139.7 (C), 133.7 (C), 132.6 (C), 131.5 (CH), 131.1 (C), 130.7 (CH), 128.53 (CH), 128.49 (CH), 128.4 (CH), 123.4 (C), 121.6 (CH), 116.4 (C), 96.6 (C), 81.9 (C), 17.7 (CH_3), 16.7 (CH_3), 16.7 (CH_3), 14.8 (two CH_3), 14.2 (CH_3) ppm. ^{11}B NMR ($CDCl_3$, 160 MHz) δ 0.69 (t, $J_{B\text{-}F}$ = 33.1 Hz), 0.34 (s) ppm. ^{19}F NMR ($CDCl_3$, 471 MHz) δ -146.7 (q, $J_{B\text{-}F}$ = 30.7 Hz) ppm. FTIR ν 1712, 1548, 1464, 1198 cm^{-1}. HRMS (ESI$^+$) *m/z* $[M + Na]^+$ Calcd. for $C_{70}H_{61}B_3F_4N_6NaO_4$ 1181.4867, Found 1181.4888.

3. ^{1}H, ^{13}C, ^{11}B and ^{19}F NMR spectra of new compounds

^{1}H NMR (THF-d_8, 300 MHz) of 3

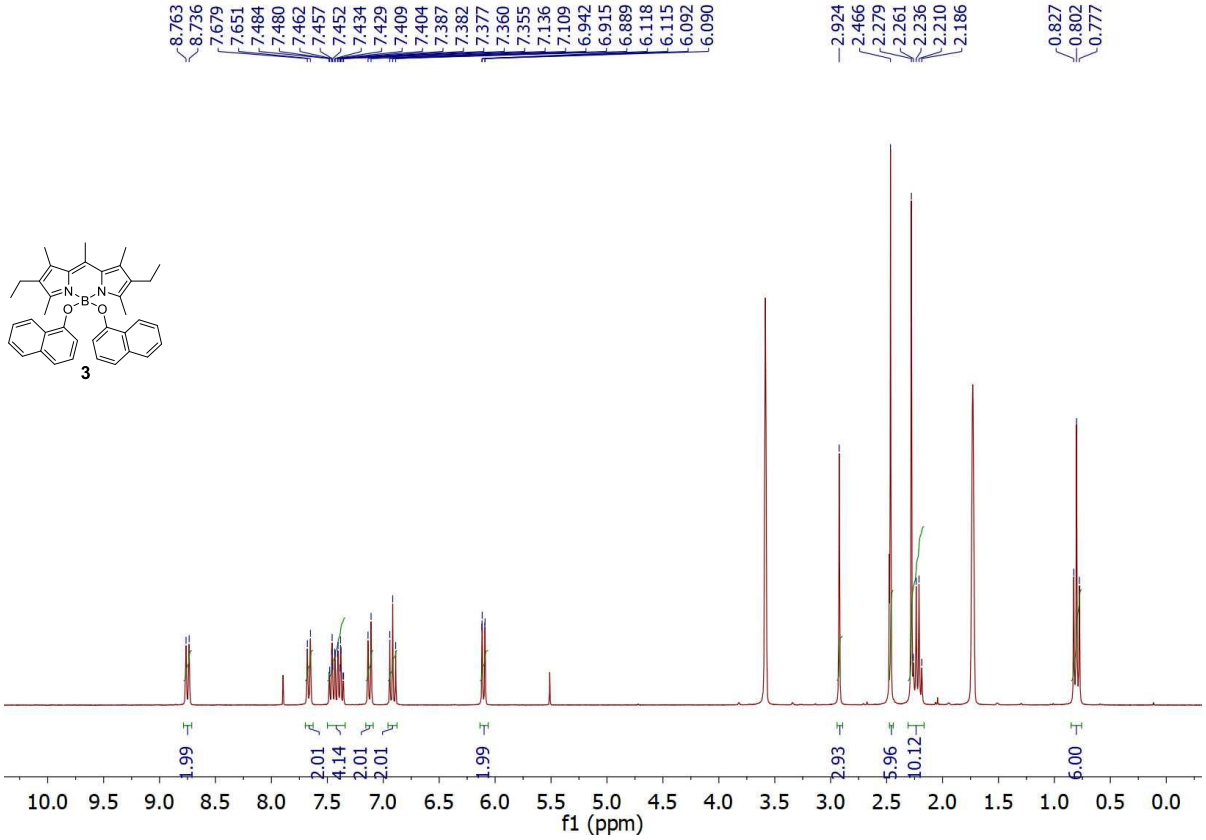

^{13}C NMR (THF-d_8, 75 MHz) of 3

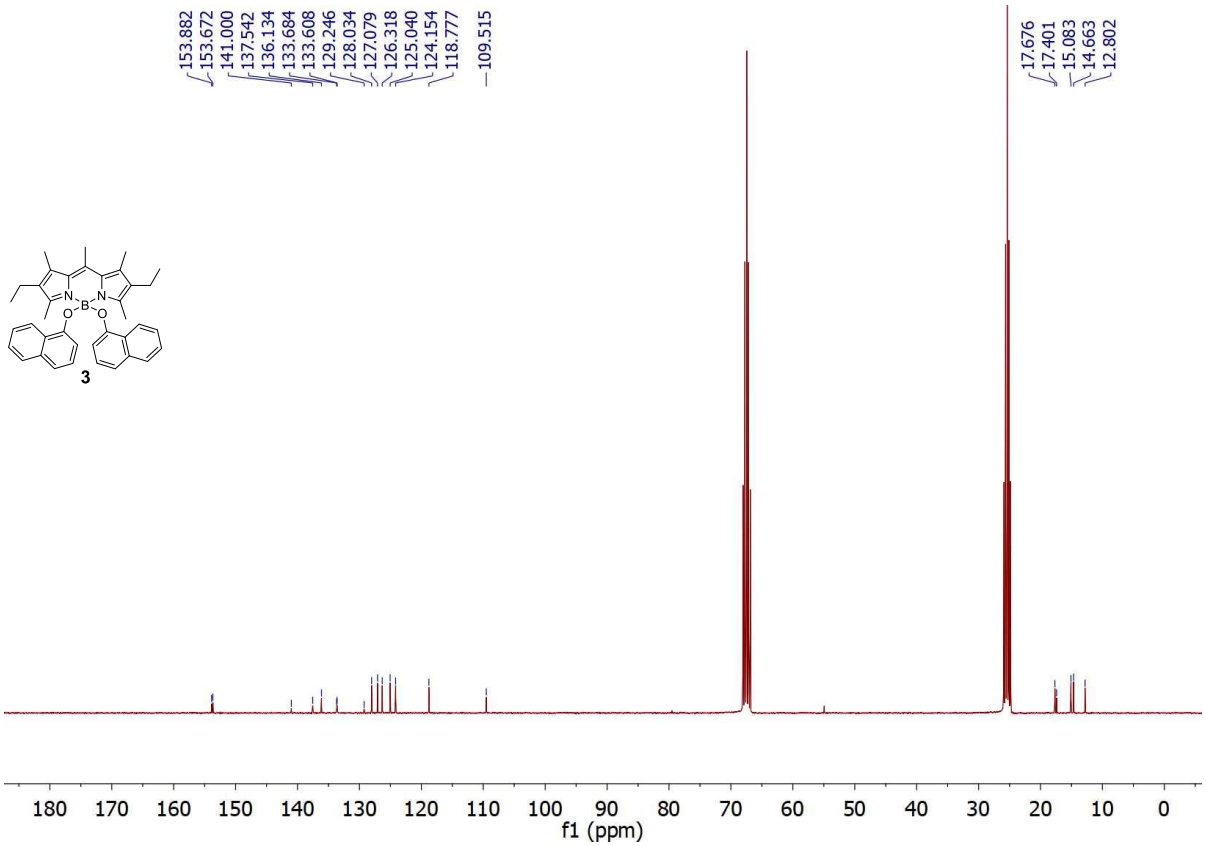

^{11}B NMR (THF-d_8, 160 MHz) of 3

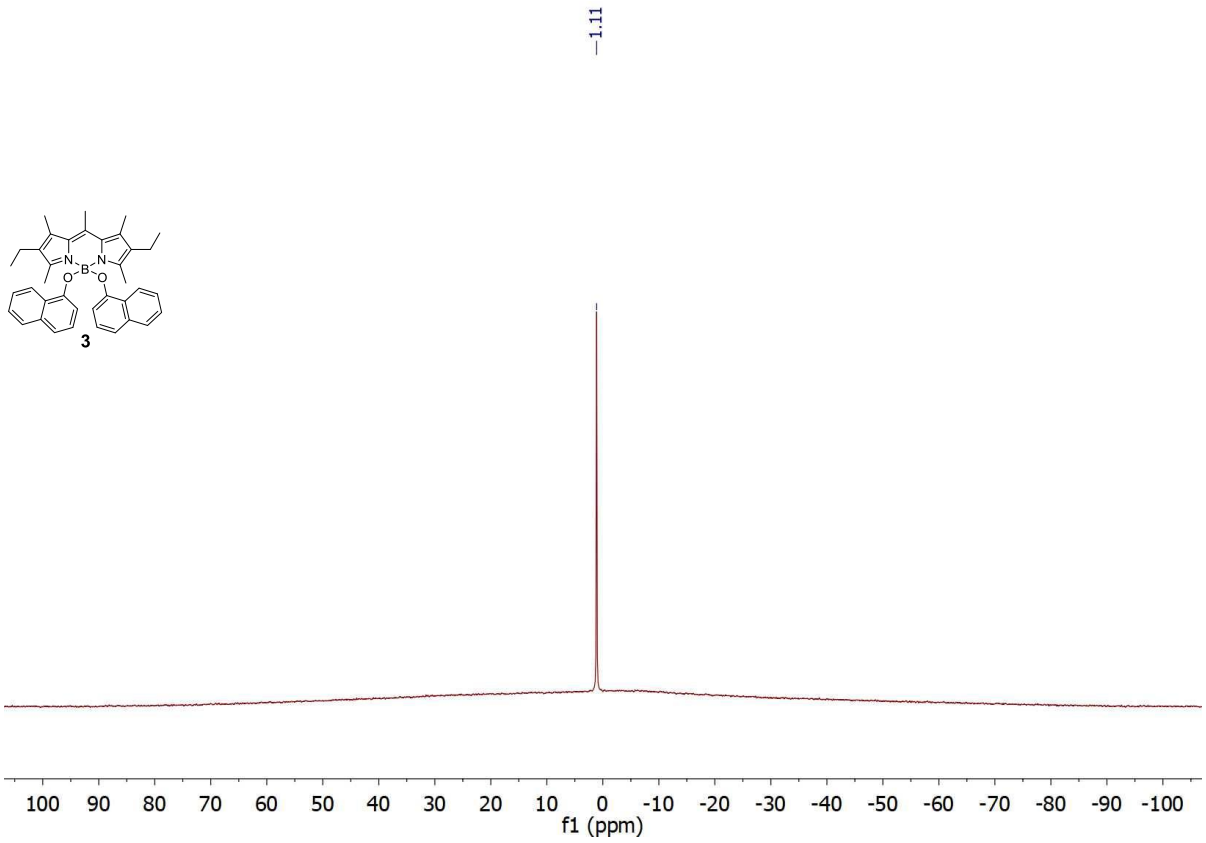

^{1}H NMR ($CDCl_3$, 300 MHz) of 4a

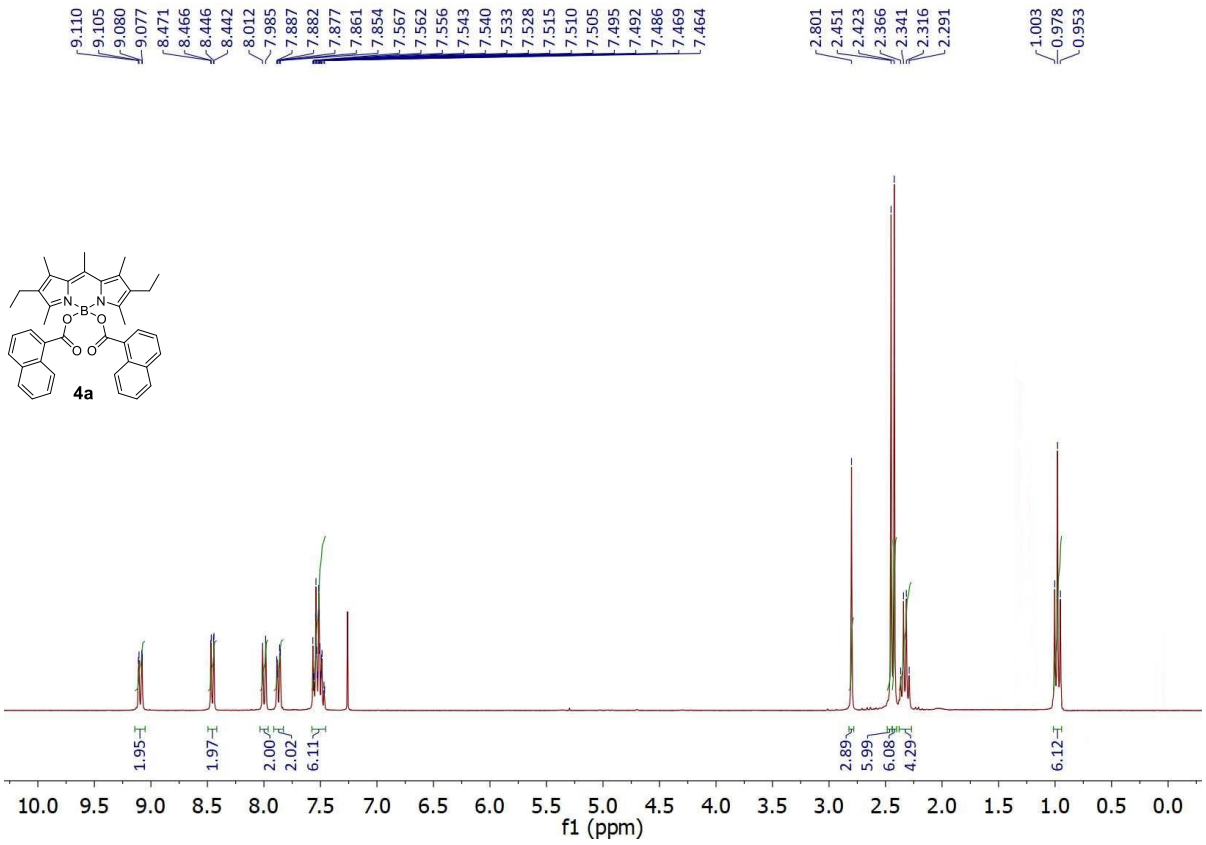

^{13}C NMR ($CDCl_3$, 75 MHz) of 4a

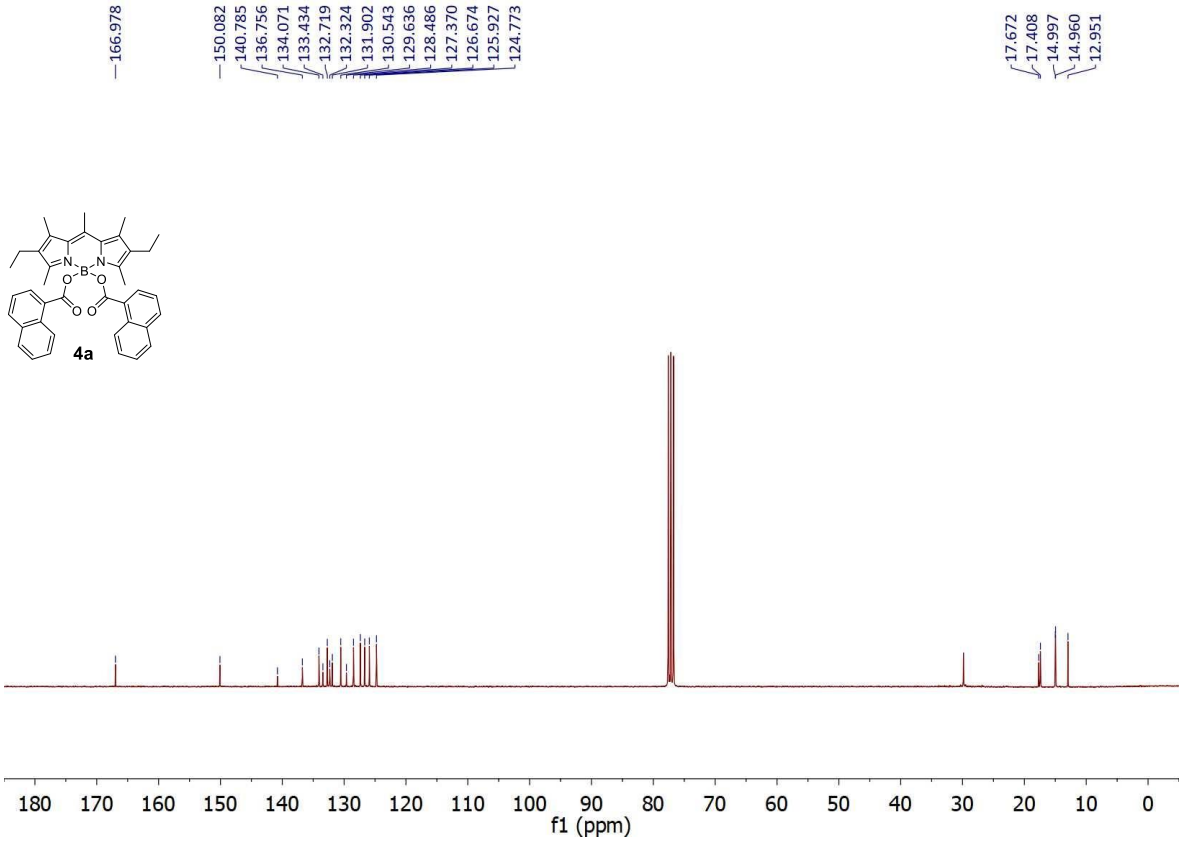

^{11}B NMR ($CDCl_3$, 160 MHz) of 4a

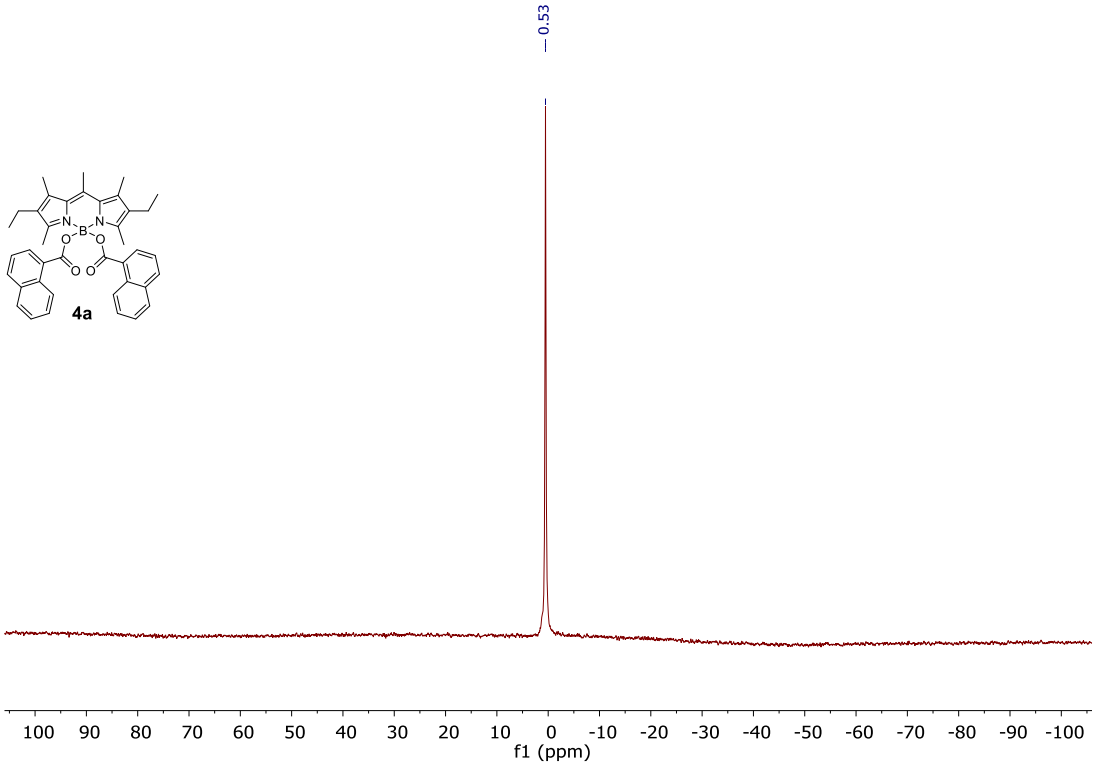

^{1}H NMR ($CDCl_3$, 300 MHz) of 4b

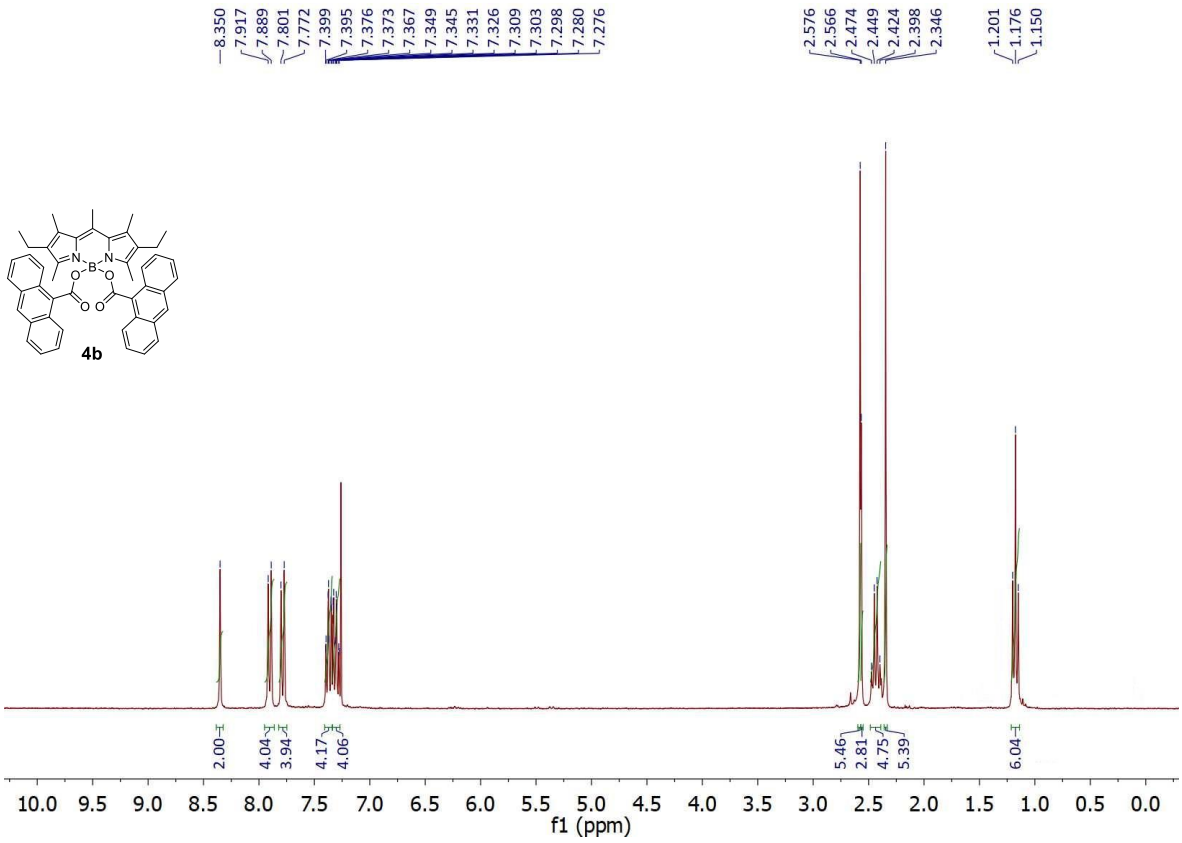

^{13}C NMR ($CDCl_3$, 75 MHz) of 4b

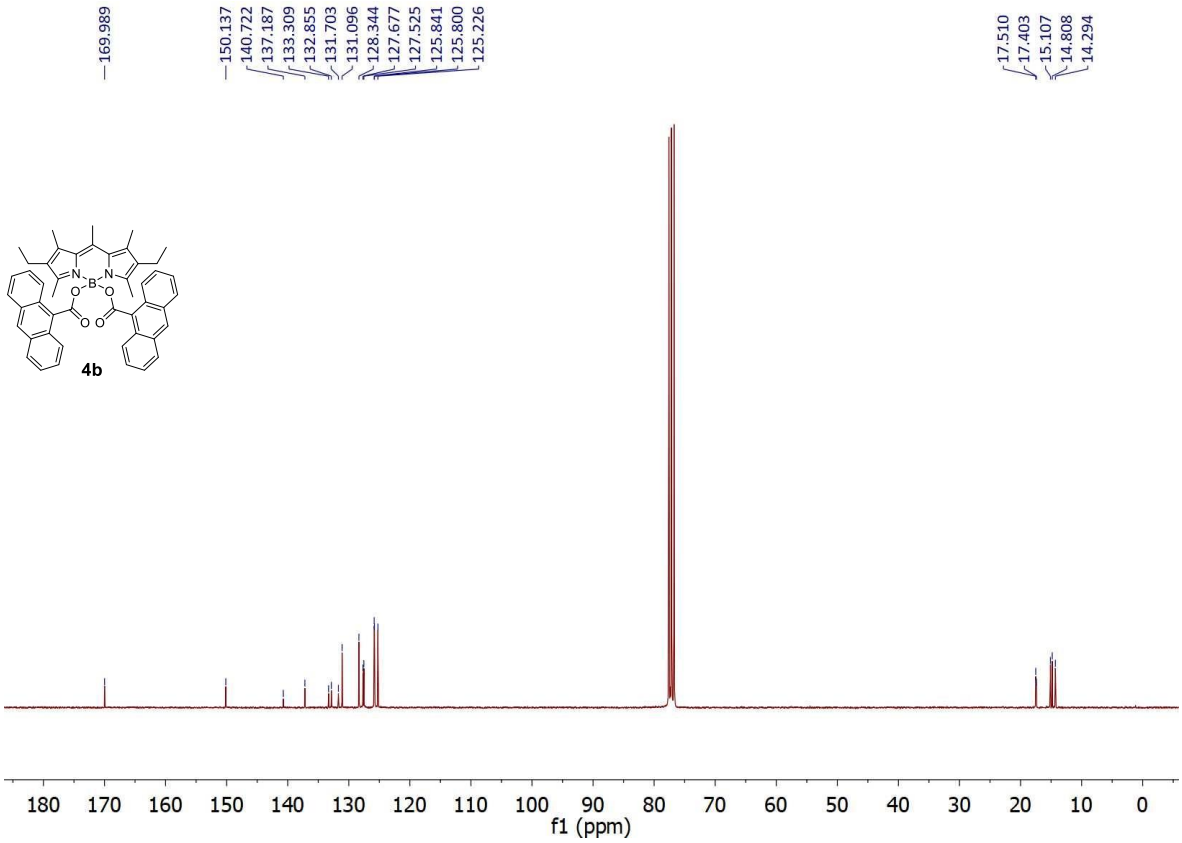

^{11}B NMR ($CDCl_3$, 160 MHz) of 4b

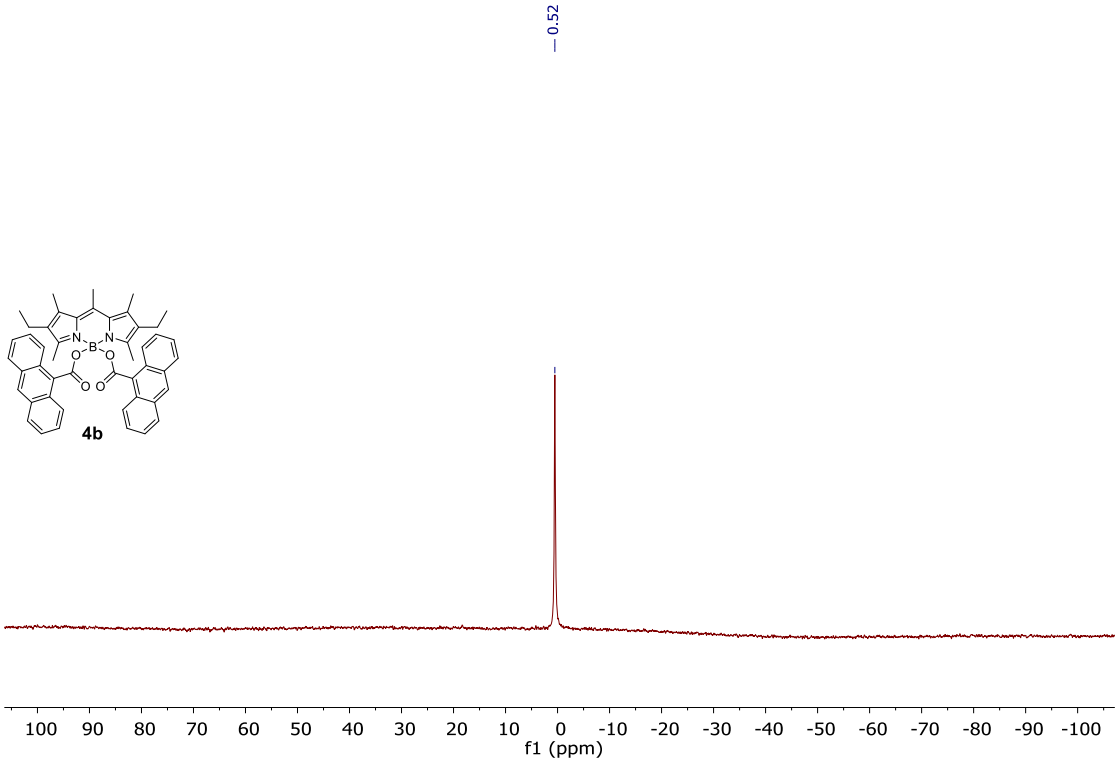

^{1}H NMR ($CDCl_3$, 500 MHz) of 4c

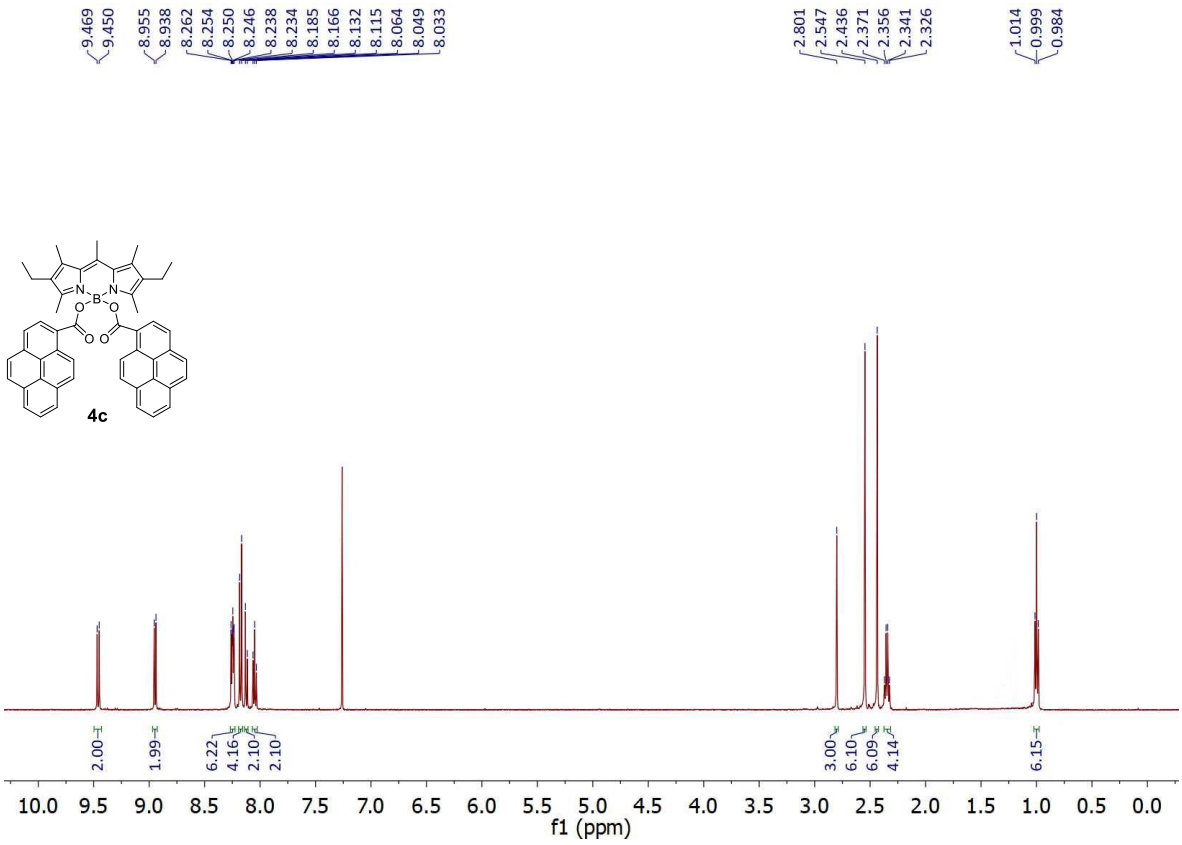

^{13}C NMR ($CDCl_3$, 75 MHz) of 4c

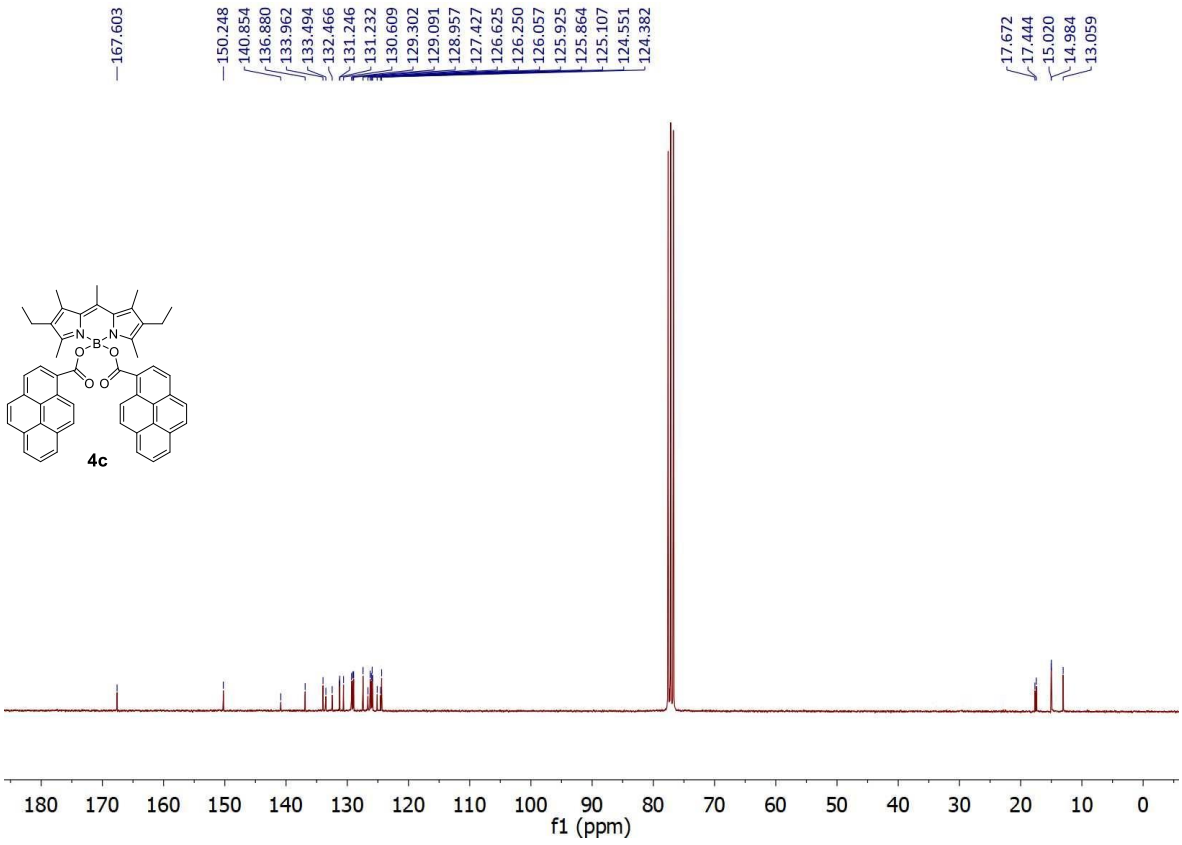

^{11}B NMR ($CDCl_3$, 160 MHz) of 4c

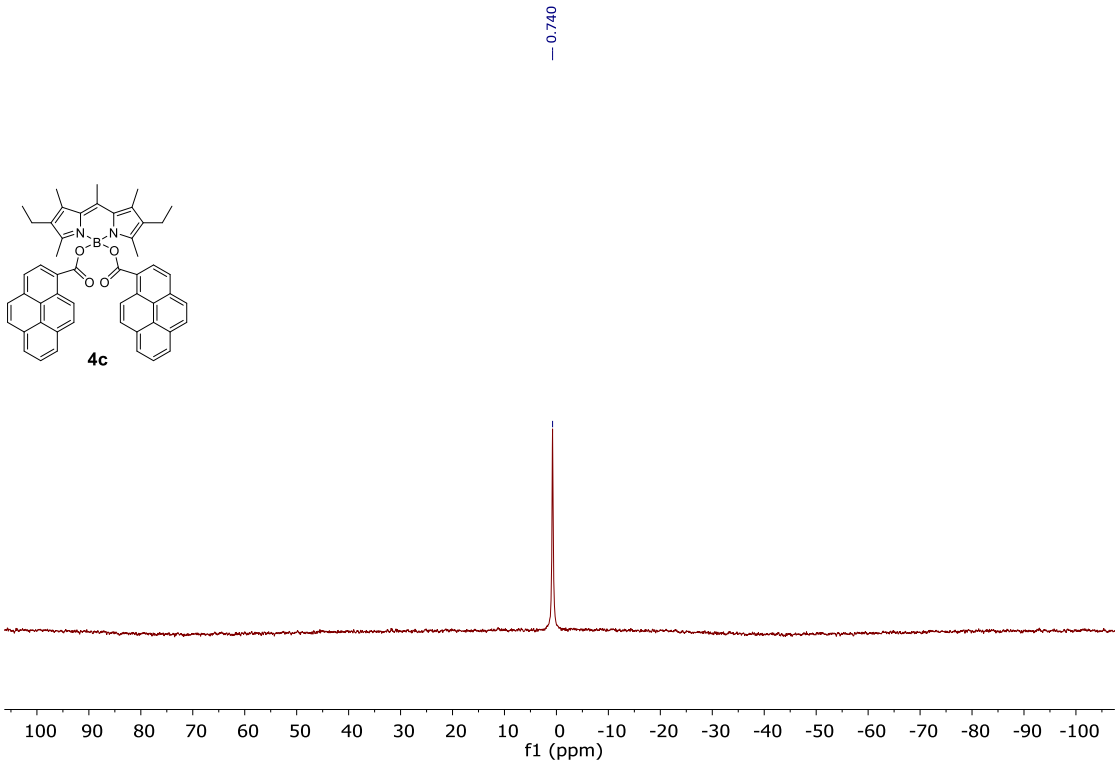

^{1}H NMR ($CDCl_3$, 300 MHz) of 4d

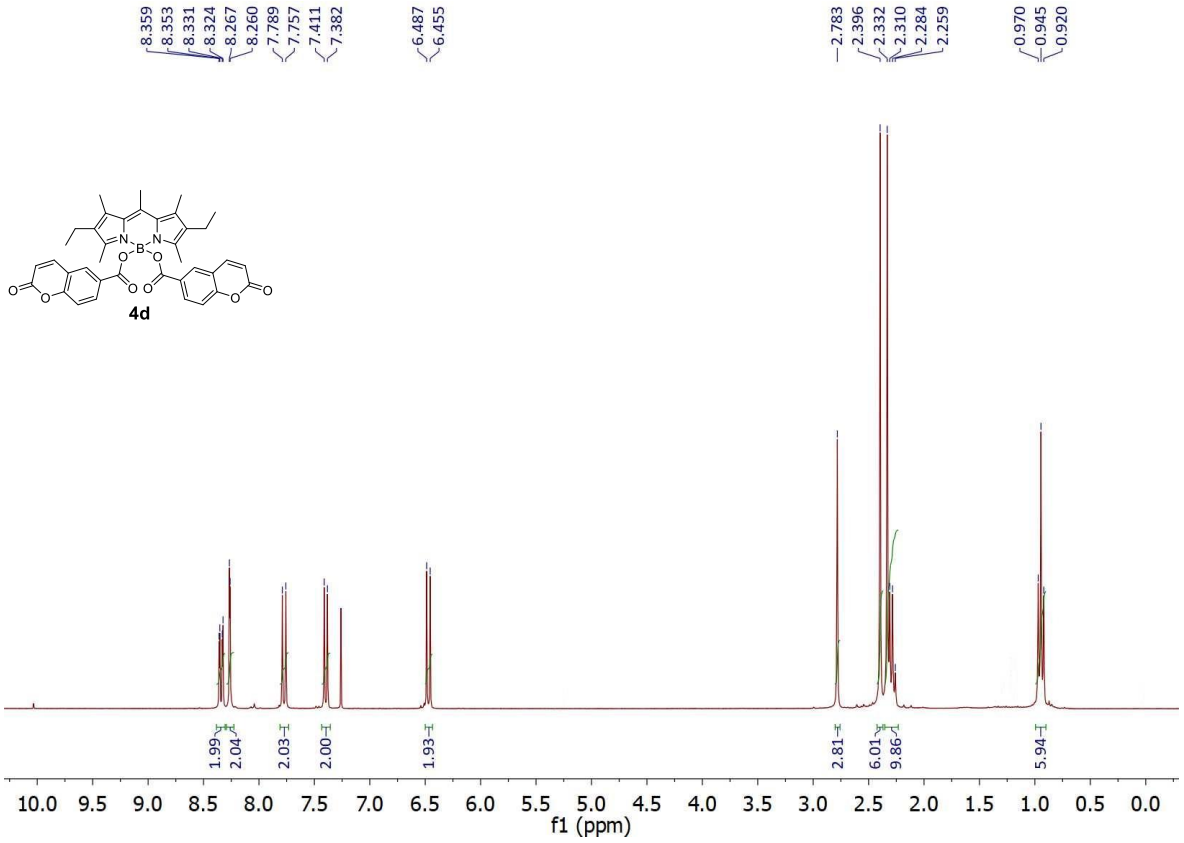

^{13}C NMR ($CDCl_3$, 75 MHz) of 4d

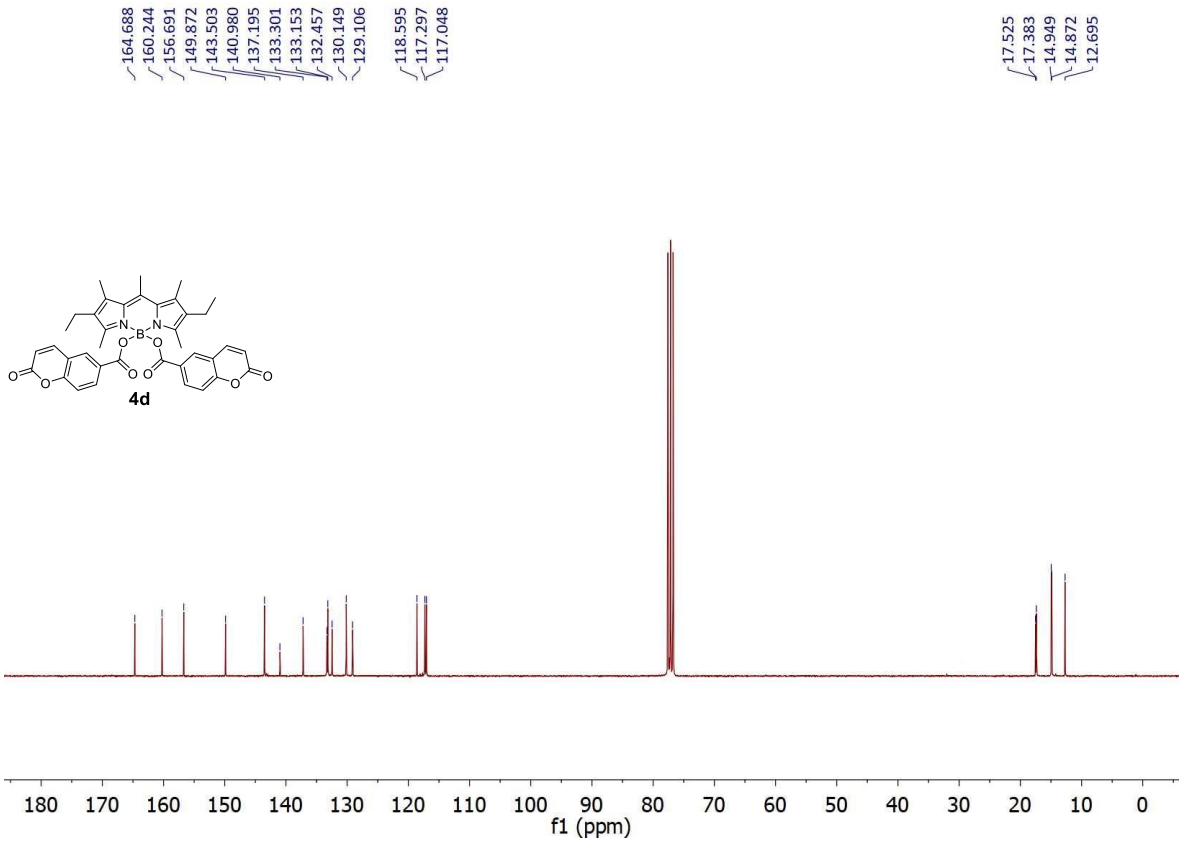

^{11}B NMR ($CDCl_3$, 160 MHz) of 4d

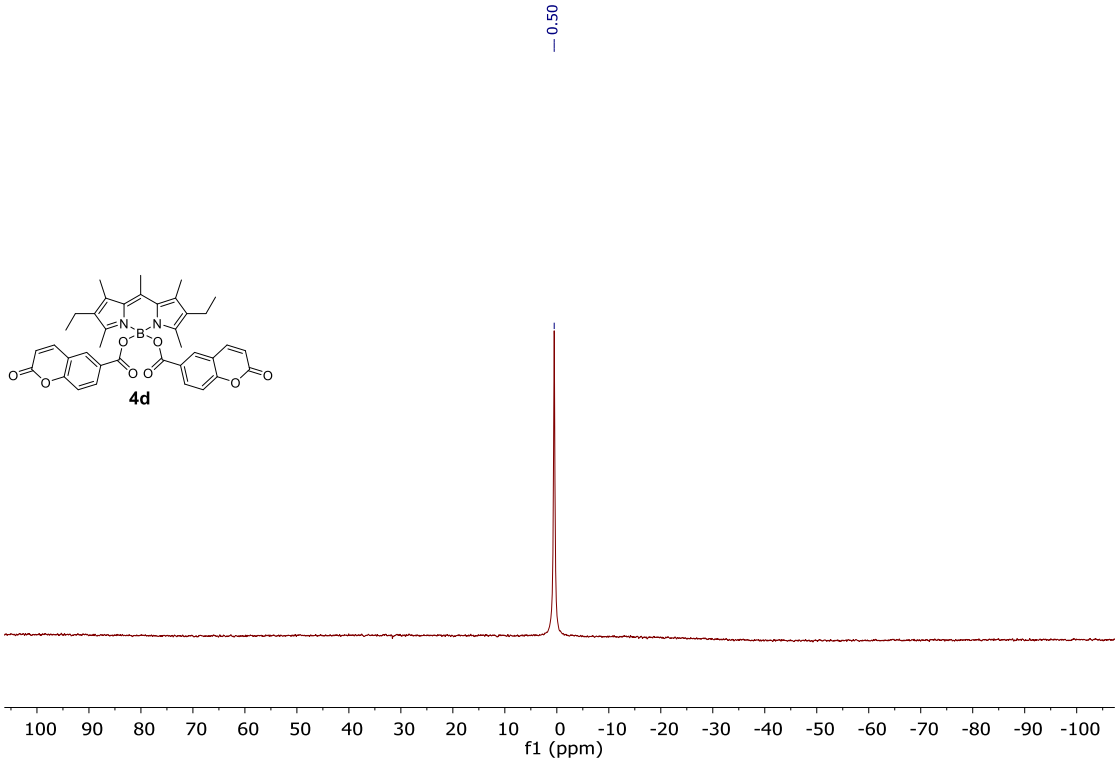

^{1}H NMR ($CDCl_3$, 300 MHz) of 4f

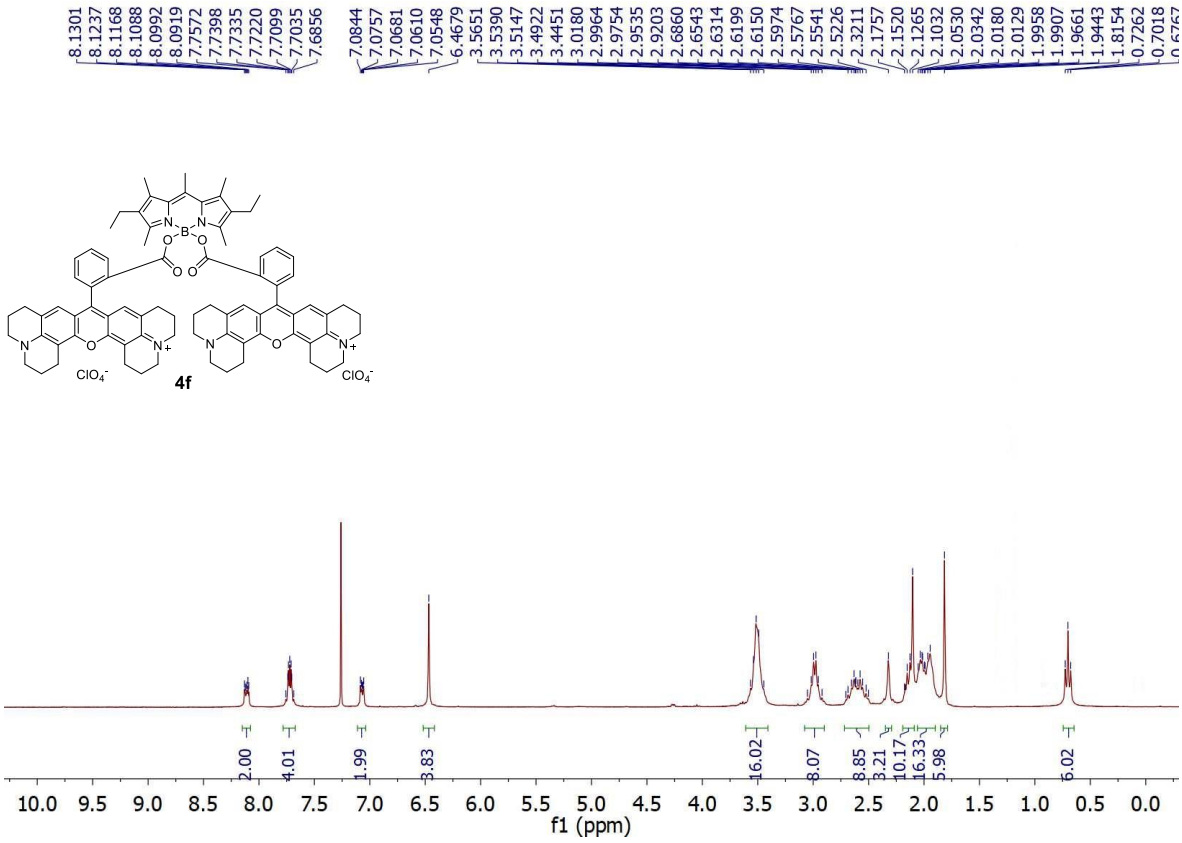

^{13}C NMR ($CDCl_3$, 75 MHz) of 4f

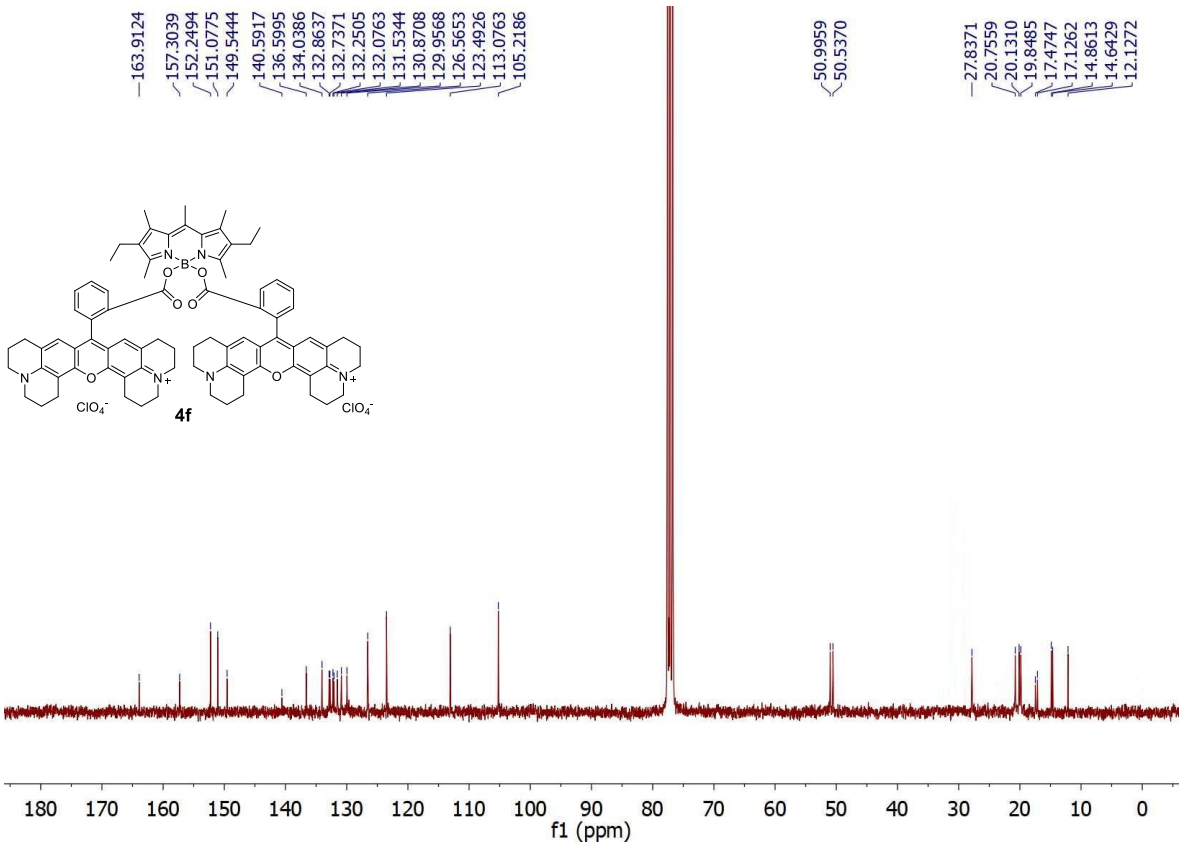

^{11}B NMR ($CDCl_3$, 160 MHz) of 4f

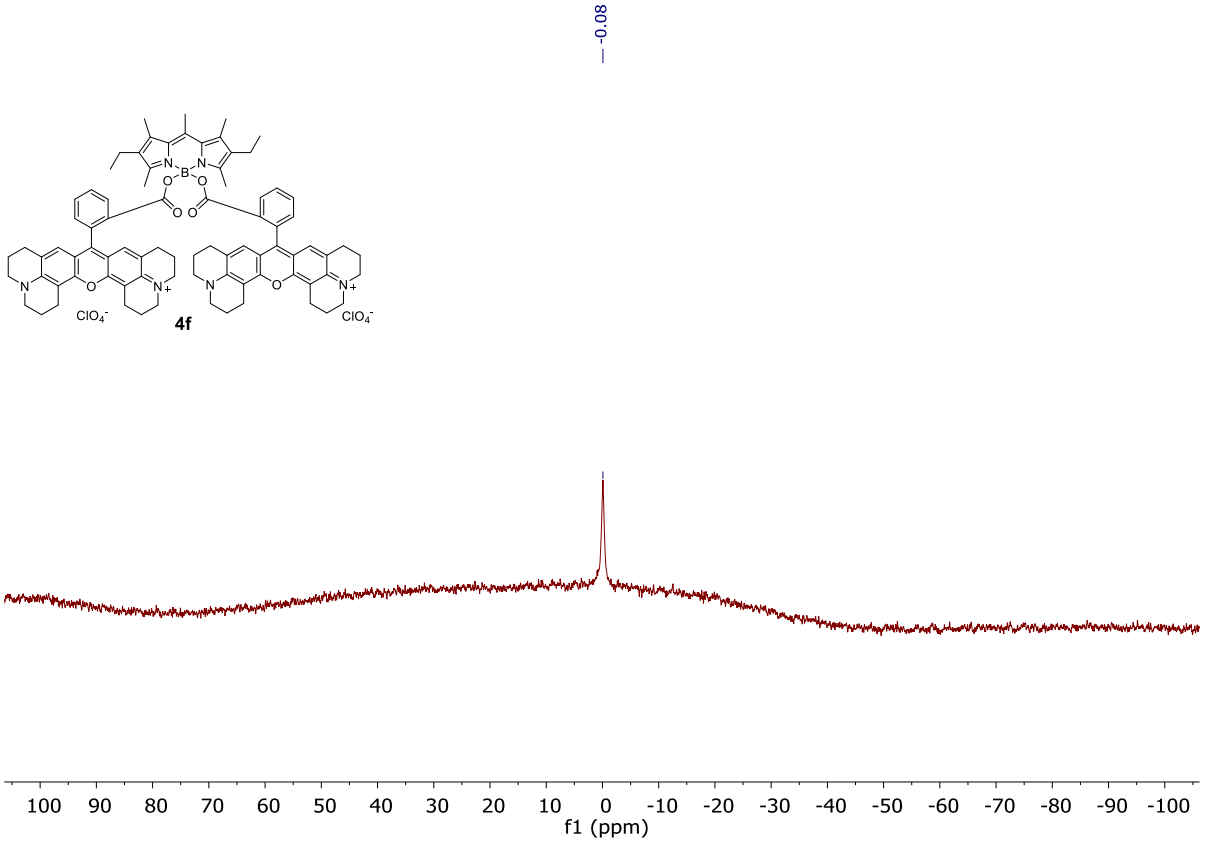

^{1}H NMR ($CDCl_3$, 300 MHz) of 5c

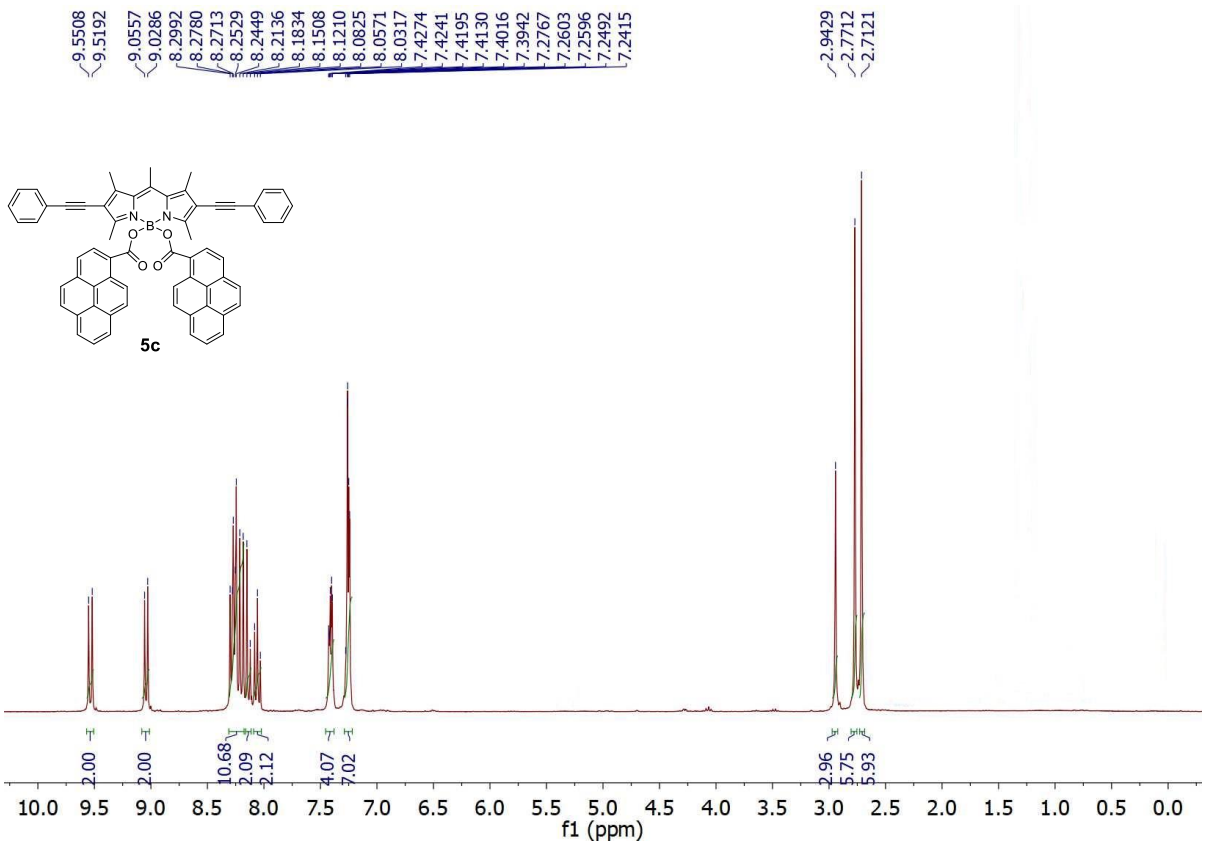

^{13}C NMR ($CDCl_3$, 75 MHz) of 5c

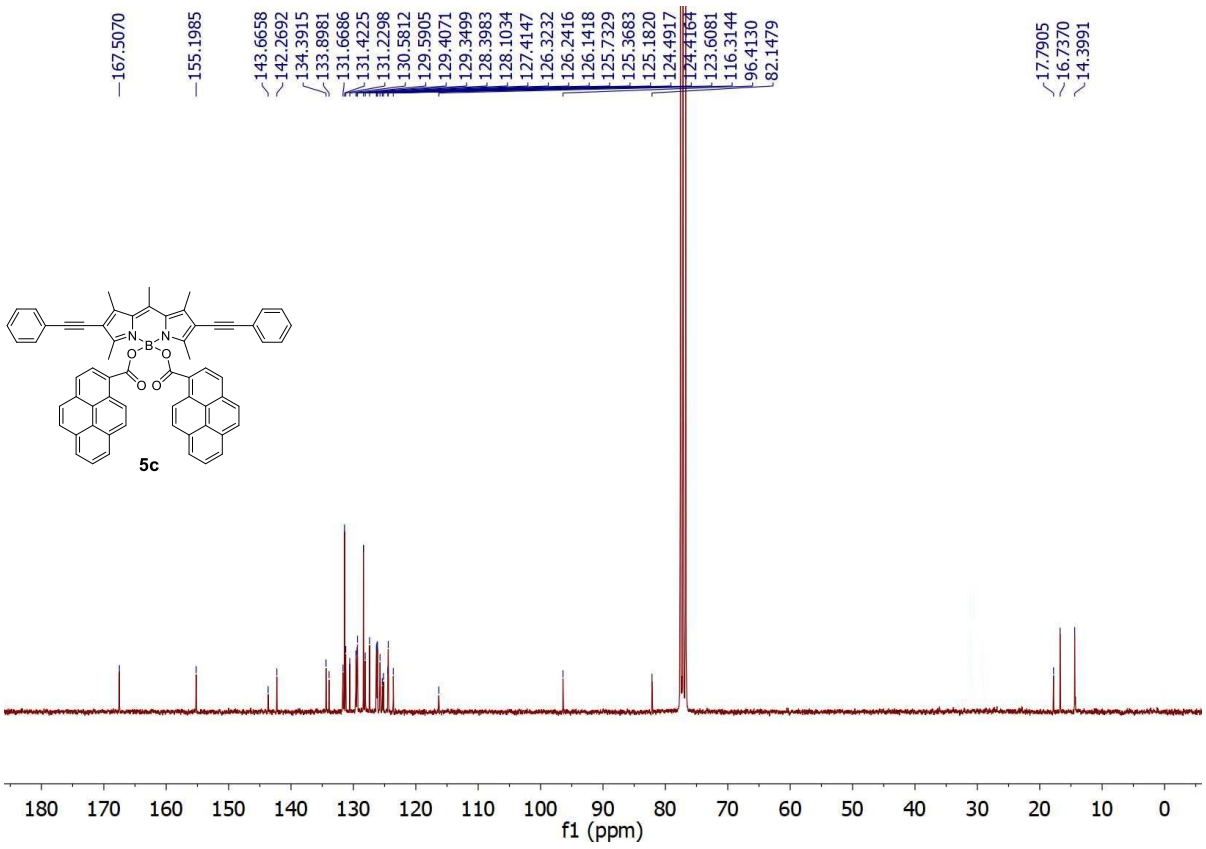

^{11}B NMR ($CDCl_3$, 160 MHz) of 5c

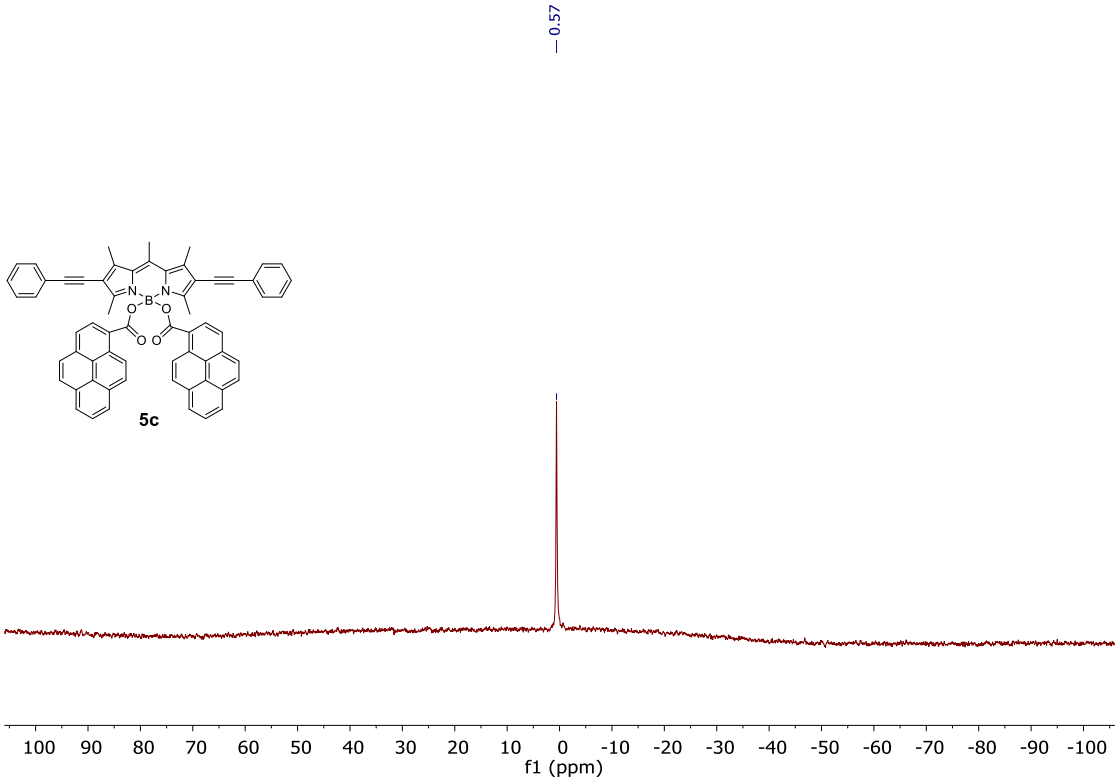

^{1}H NMR ($CDCl_3$, 700 MHz) of 5e

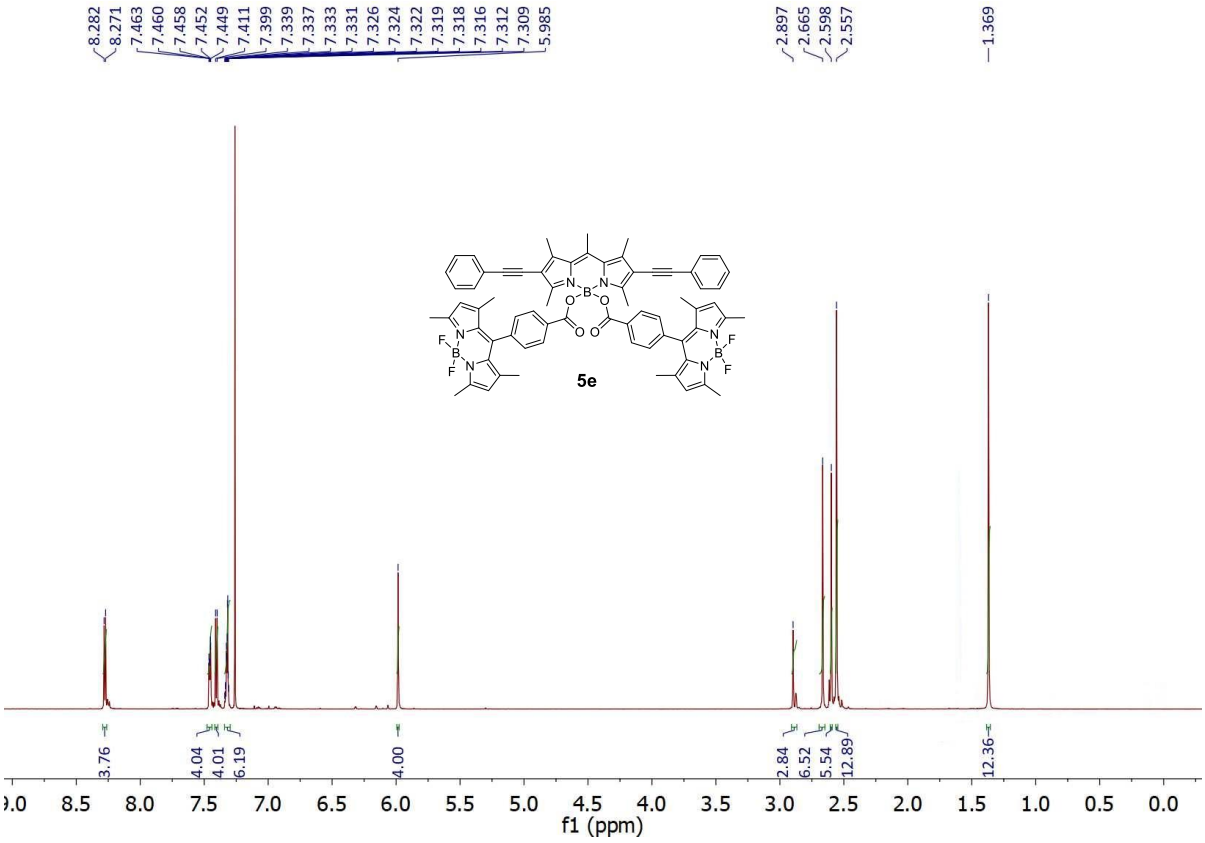

^{13}C NMR ($CDCl_3$, 176 MHz) of 5e

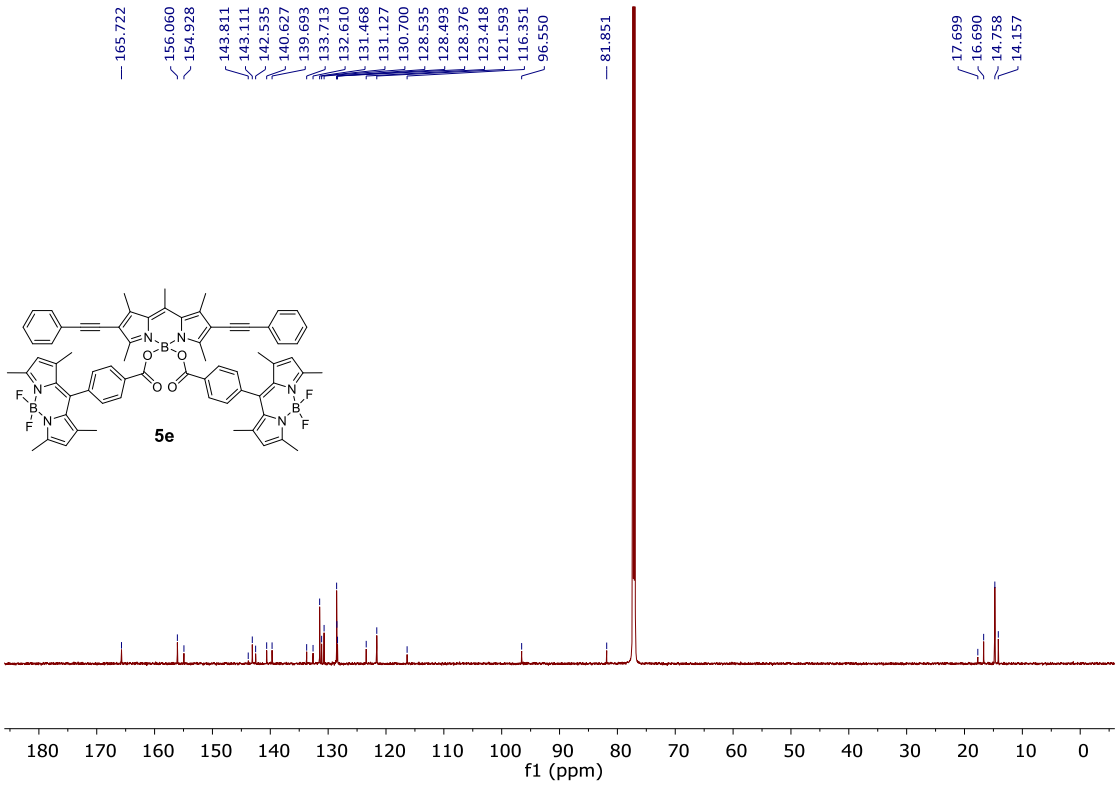

^{11}B NMR ($CDCl_3$, 160 MHz) of 5e

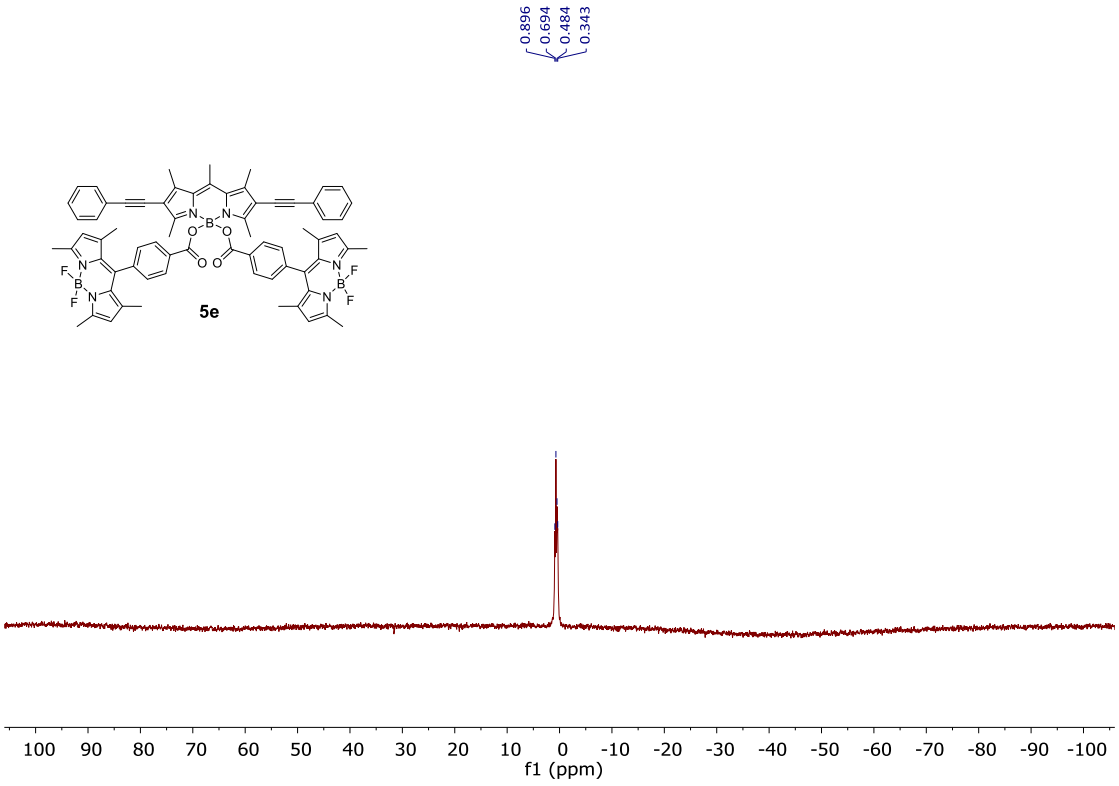

^{19}F NMR ($CDCl_3$, 471 MHz) of 5e

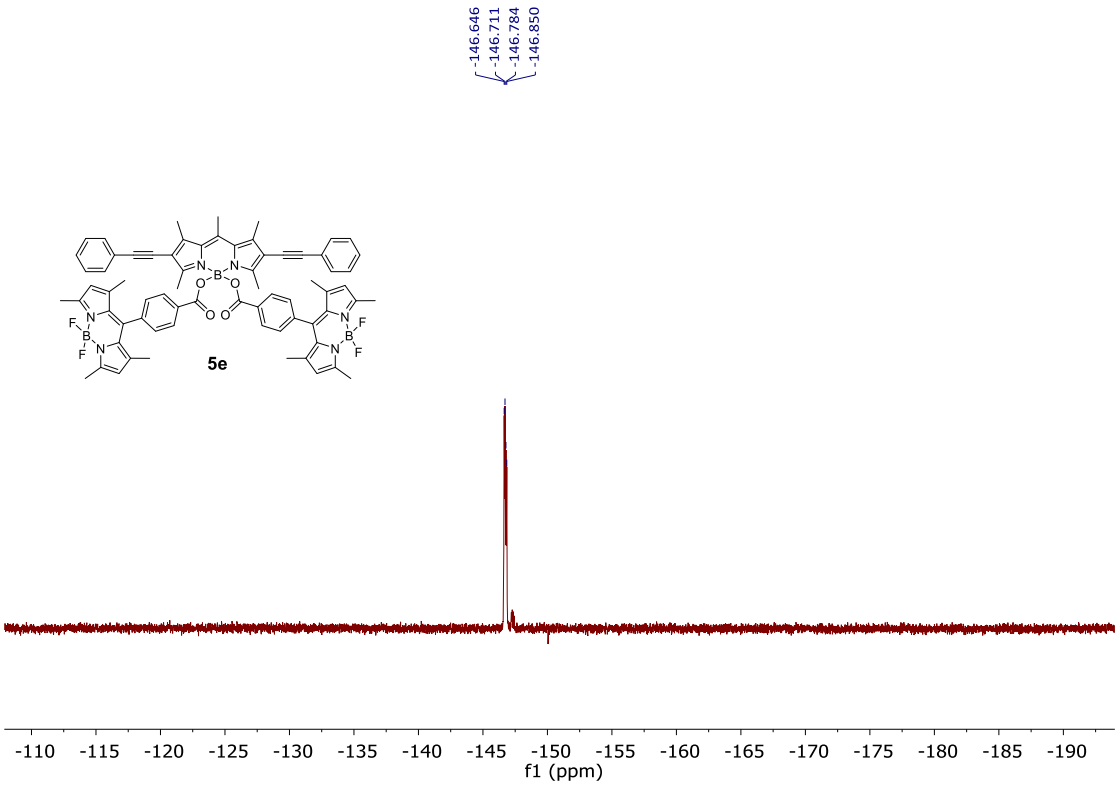

4. Phtophysical and lasing properties

Table S1. Photophysical properties of *O*-BODIPY-based MMA **3** *COO*-BODIPY-based MMAs **4a-d**, **4f** and **5c,e** in solution (2 μM) of solvents representative of apolar and polar media.

Dye solvent	λ_{ab} [a] **(nm)**	ε_{max} [b] **(10^4 M^{-1}·cm^{-1})**	λ_{fl} [c] **(nm)**	ϕ [d]	τ [e] **(ns)**	k_{fl} [f] **($10^8 s^{-1}$)**	k_{nr} [g] **($10^8 s^{-1}$)**	***EETE*** [h]
3								
c-hex	524.5	7.5	541.0	0.03	0.44 (68%) 5.33 (32%)			95
EtOAc	519.5	7.0	536.0	0.01	0.19 (92%) 5.36 (8%)			95
ACN	517.0	6.5	532.5	0.02	0.15 (94%) 5.39 (6%)			95
4a								
c-hex	524.5	7.5	541.5	0.82	6.18	1.33	0.29	98
EtOAc	520.5	6.1	536.0	0.80	6.58	1.21	0.31	98
ACN	520.0	5.8	536.5	0.82	7.10	1.16	0.25	98
4b								
c-hex	526.0 (363)	4.5 (1.7)	547.5	0.94	7.39 [i]	1.27	0.08	98
EtOAc	523.0 (382)	6.0 (2.8)	547.0	0.80	7.83 [i]	1.02	0.25	99
ACN	524.5 (364)	4.3 (2.5)	549.0	0.70	9.20 [i]	0.76	0.32	99
4c								
c-hex	524.5 (355)	7.2 (5.8)	540.5	0.83	6.21	1.34	0.27	98
EtOAc	520.5 (354)	6.4 (6.3)	537.0	0.86	6.51	1.32	0.22	98
ACN	520.0 (348)	5.8 (5.6)	539.5	0.88	6.86 [i]	1.28	0.17	98
4d								
THF	522.0	7.4	537.5	0.82	6.27	1.31	0.29	98
EtOAc	520.5	6.9	537.0	0.82	6.46	1.26	0.28	98
ACN	519.5	6.5	535.5	0.88	6.77	1.30	0.17	98
4f								
EtOAc	578.5 (513)	6.7 (6.2)	598.5	0.07	0.20 (59%) 0.80 (27%) 4.02 (14%)			97
ACN	577.0 (511)	9.5 (8.6)	593.0	0.08	0.13 (44%) 0.44 (44%) 4.39 (12%)			97
5c								
c-hex	564.0 (356)	4.2 (3.2)	589.0	0.85	4.23	2.02	0.34	95
EtOAc	556.5 (355)	6.2 (6.4)	587.0	0.56	4.26	1.32	1.03	95
ACN	556.5 (354)	4.2 (4.0)	592.5	0.54	4.01	1.35	1.14	95
5e								
c-hex	562.5 (502)	6.5 (20.4)	588.5	0.66	4.78	1.38	0.71	97
EtOAc	557.5 (499)	5.6 (19.1)	591.0	0.57	4.62	1.24	0.93	99
ACN	555.0 (497)	4.4 (17.7)	590.5	0.43	4.16	1.03	0.71	99

[a]Absorption wavelength; [b]Extinction coefficient of the main maxima; [c]Fluorescence wavelength; [d]Fluorescence quantum yield; [e]Fluorescence lifetime (independent of the excitation); [f]Radiative rate constant; [g]Non-radiative rate constant; [h]Excitation energy transfer efficiency (%); [i]Amplitude-average lifetime of the biexponential fit with two long-lifetime components (around 2-4 the minor one and 8-9 the major one). c-hex: cyclohexane. EtOAc: ethyl acetate. ACN: acetonitrile. THF: tetrahydrofuran.

Table S2. Lasing efficiencies exhibited by *COO*-BODIPY-based MMAs **4a-d**, **4f** and **5c,e** when transversely pumped at 532 nm or 355 nm in ethyl acetate solution (Eff_{532} and Eff_{355}, respectively), as well as wavelength of the obtained laser peak (λ_{las}). Corresponding data from *O*-BODIPY MMA (**3**) and laser dye PM567 pumped under otherwise identical experimental conditions are included for comparison purposes.

Dye	Eff_{532} (%)	Eff_{355} (%)	λ_{las} (nm)
PM567	48	33	566
3	26	19	563
4a	64	50	564
4b	60	48	567
4c	63	57	563
4d	62	53	560
4f	16	9	616
5c	65	55	598
5e	50	38	607

Table S3. Theoretically calculated molecular dipole moments (in Debyes) in the ground (S_0, wb97xd/6-311g*) and first excited (S_1, td wb97xd/6-311g*) state for MMAs **3**, **4a-d**, **4f** and **5c,e**. For larger MMA **4f**, the calculation in the excited state was computationally not available (NA).

Dye	μ (S_0) *(Debyes)*	μ (S_1) (Debyes)
3	4.71	4.78
4a	5.99	6.10
4b	9.30	9.35
4c	9.19	9.99
4d	6.13	6.63
4f	7.25	NA
5c	8.51	8.79
5e	6.95	7.17

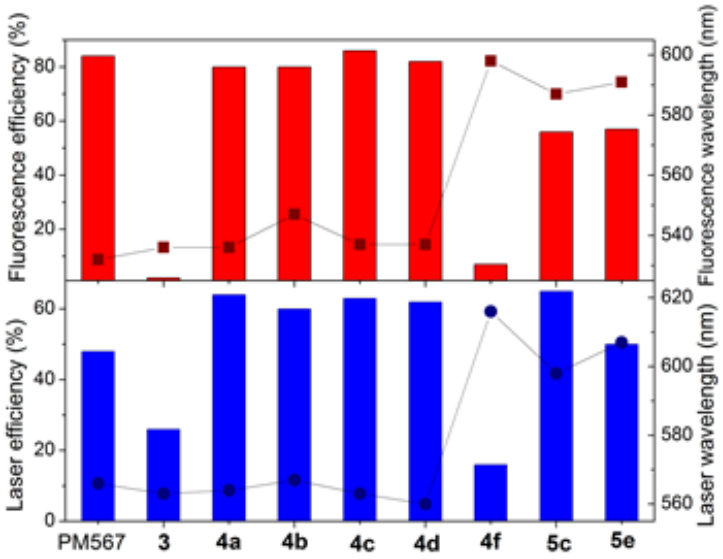

Fig. S2. Comparison of the fluorescence and laser (pumping at 532 nm) efficiency (columns) and wavelength (scatter) of MMAs **3**, **4a-d, 4f** and **5c,e** with respect to parent PM567, in ethyl acetate. For detailed data, see Table S1 (fluorescence) and Table S2 (laser)**.**

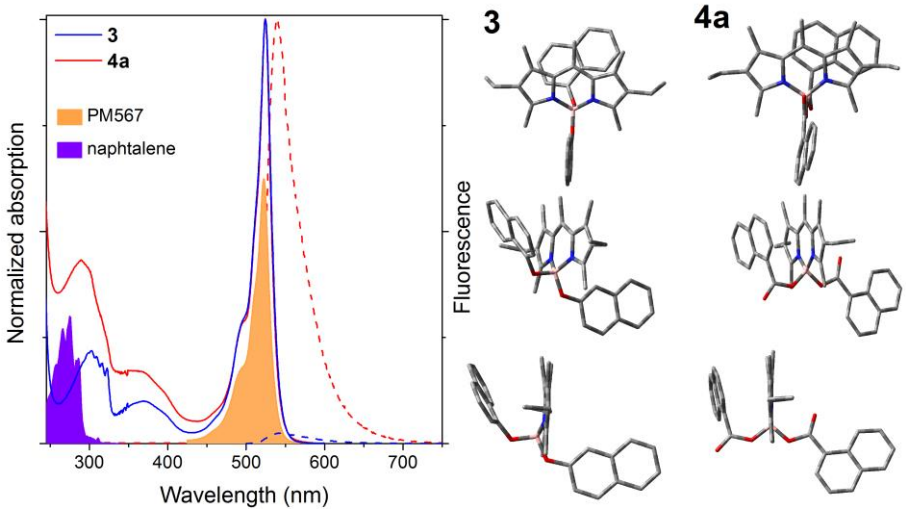

Fig. S3. Normalized UV-vis absorption (bold lines, left) and fluorescence spectra upon vis excitation (dashed lines, left) of *O*-BODIPY-based MMA **3** and *COO*-BODIPY analog **4a** in cyclohexane, and UV-vis absorption spectra of the monochromophoric dyes PM567 and naphthalene in cyclohexane (filled spectra, left), as well as ground-state optimized geometries of **3** and **4a** (wb97xd/6-311g*, right). The computed geometries highlight the different spatial arrangement of the pendant naphthalene chromophores in both dyes and the distortion of the BODIPY chromophore in **3**. Note the disposition of the boron atom (out of the dipyrrin plane) in the bottom ground-state perspective of **3**, but not in **4a** (computed deviations *ca.* 33º and <1.5º, respectively).

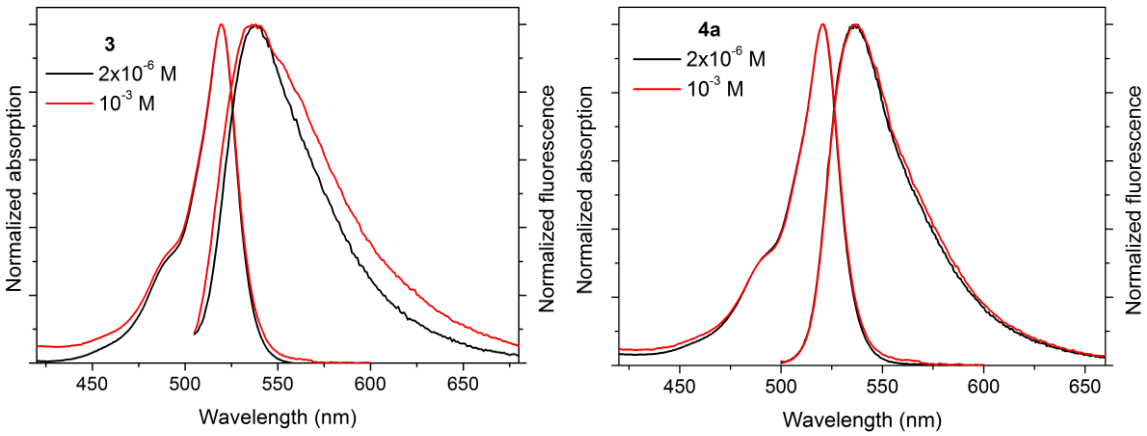

Fig. S4. Normalized absorption and fluorescence spectra of *O*-BODIPY-based MMA **3** and *COO*-BODIPY analog **4a** at different dye concentrations in ethyl acetate.

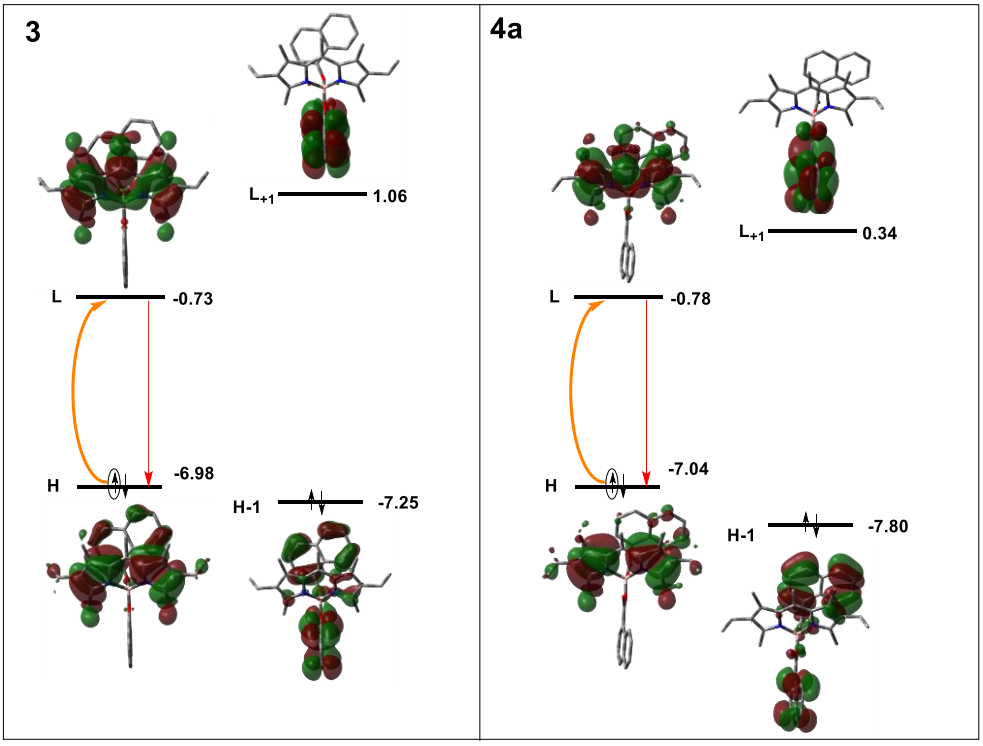

Fig. S5. Computed (wb97xd/6-311g*) contour maps and energies (in eV) of key molecular orbitals involved in the main UV-vis transitions in *O*-BODIPY-based MMA **3** and *COO*-BODIPY-based **4a,** both based on naphthalene.

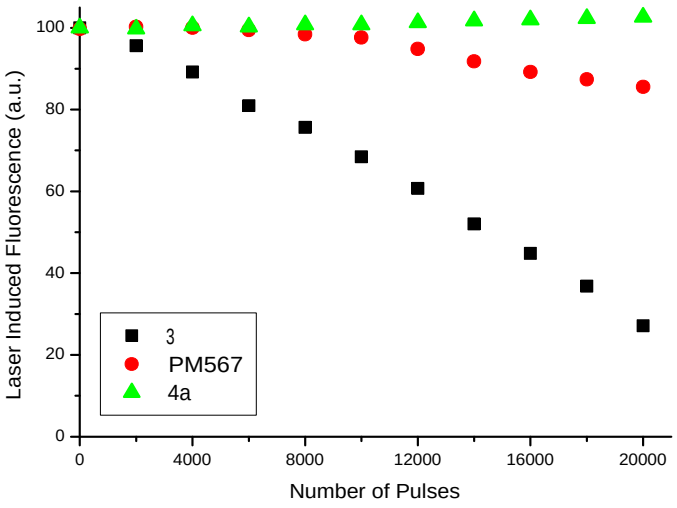

Fig. S6. Variation of the laser-induced fluorescence (LIF) intensity (relative to the initial LIF intensity in percentage terms) of *O*-BODIPY MMA **3**, *COO*-BODIPY MMA **4a** and parent commercial laser-dye PM567 with respect to the number of pumping pulses (laser-source wavelength: 532 nm; pulse duration: 8 ns; pulse energy: 5 mJ; pulse rate 15 Hz). *COO*-BODIPY MMAs **4b-d**, **4f** and **5c,e** exhibit the same behavior to that plotted from **4a**.

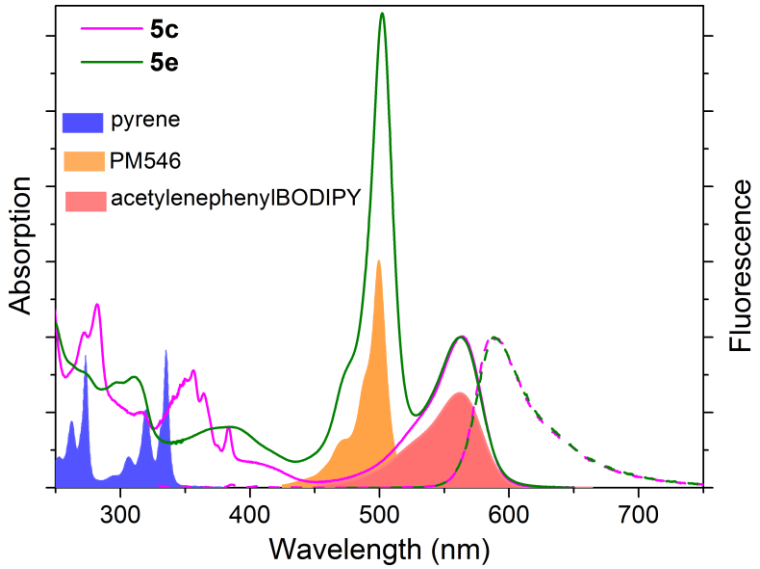

Fig. S7. Normalized UV-vis absorption spectra (bold lines) and fluorescence spectra upon UV-exciting the donor subunit pending from the boron atom (dashed lines) of 2,6-bis(phenylethynyl)BODIPY-based MMAs **5c,e** in cylclohexane, as well as UV-vis absorption spectra of the monochromophoric pyrene, PM546 (2,6-diethyl-4,4-difluoro-1,3,5,8-pentamethylBODIPY and 2,6-bis(phenylethynyl)-4,4-difluoro-1,3,5,7,8-pentamethylBODIPY (acetylenephenylBODIPY) in cyclohexane (filled spectra).

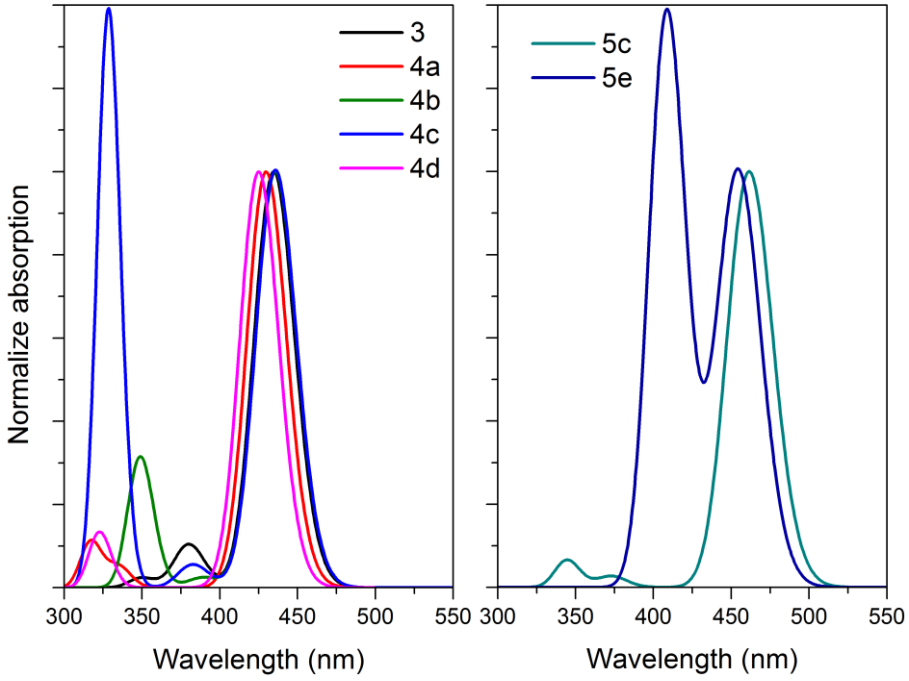

Fig. S8. Theoretically predicted (td wb97xd/6-311g*) absorption spectra (normalized by the acceptor absorption-band energy) of fluorescent MMAs **3** and **4b-d** (left) and **5c,e** (right).

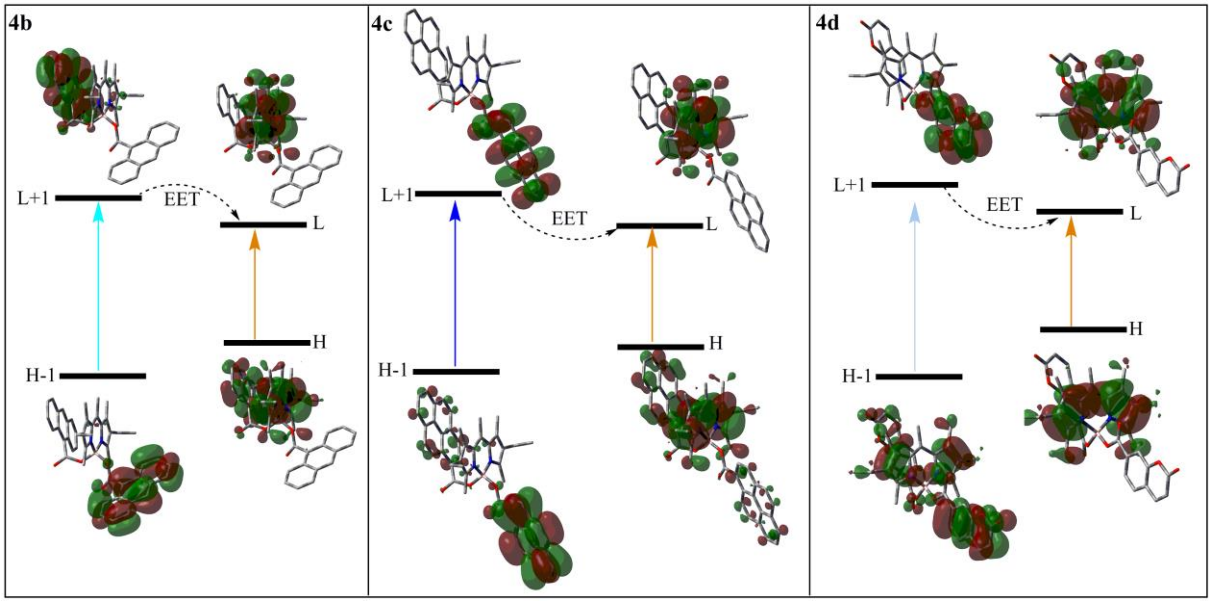

Fig. S9. Computed (wb97xd/6-311g*) contour maps and energies of the molecular orbitals involved in the main UV-vis transitions in representative PM567-derived MMAs based on anthracene (**4b**), pyrene (**4c**) and coumarin (**4d**) as the energy-donor chromophores. The corresponding HOMO-2 and LUMO+2 are just the same that the shown HOMO-1 and LUMO+1, but placed in the other energy-donor subunit (they are omitted for the sake of simplicity).

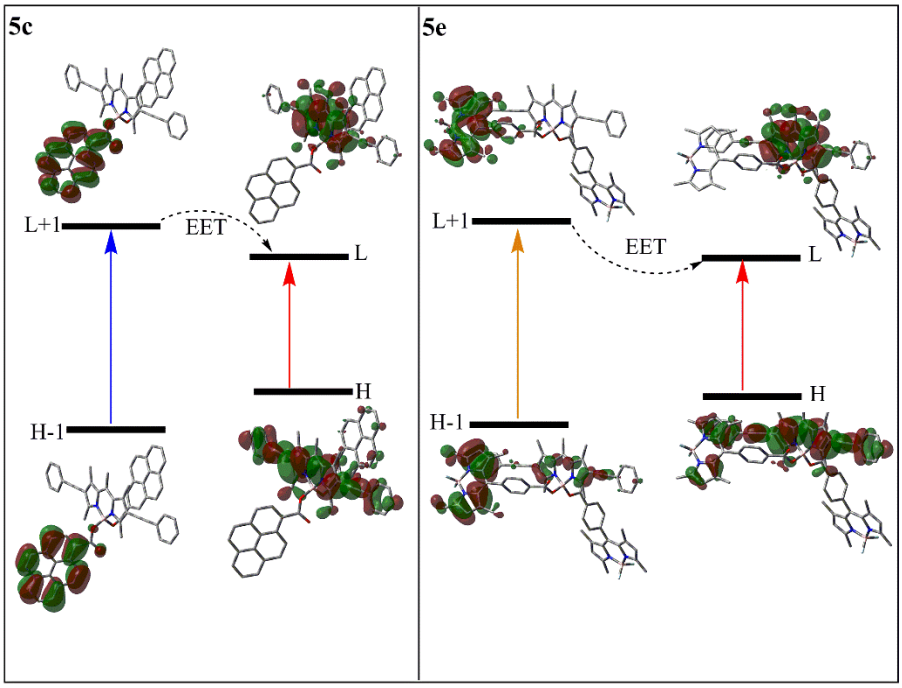

Fig. S10. Computed (wb97xd/6-311g*) contour maps and energies of the molecular orbitals (wb97xd/6-311g*) involved in the main UV-vis transitions in π-extendedBODIPY-derived MMAs based on pyrene (**5c**) or BODIPY (**5e**) as the energy-donors chromophores. The corresponding HOMO-2 and LUMO+2 are just the same that the shown HOMO-1 and LUMO+1, but placed in the other energy-donor subunit (they are omitted for the sake of simplicity).

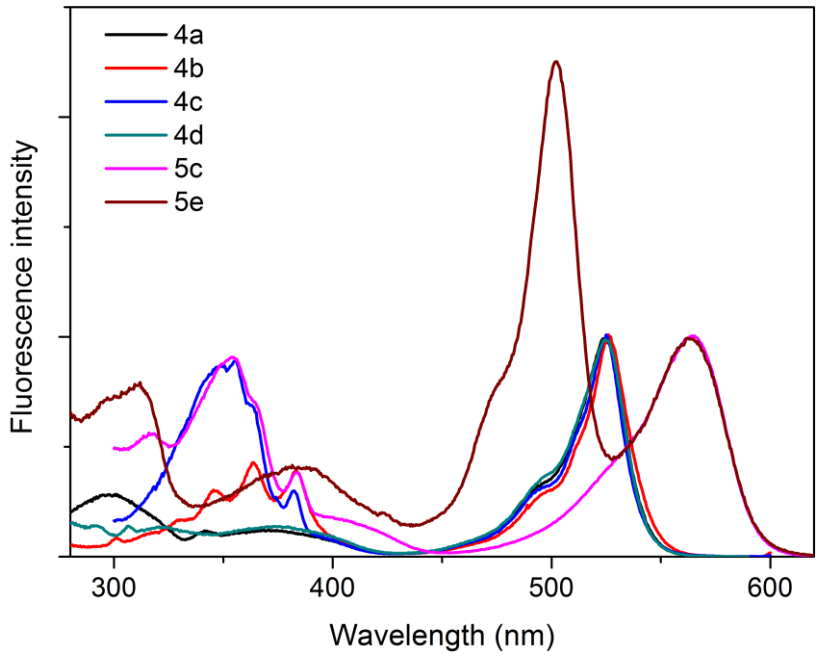

Fig. S11. Normalized excitation spectra (monitored at the emission of the energy acceptor) of MMAs **4a-d** and **5c**,**e** in cyclohexane.

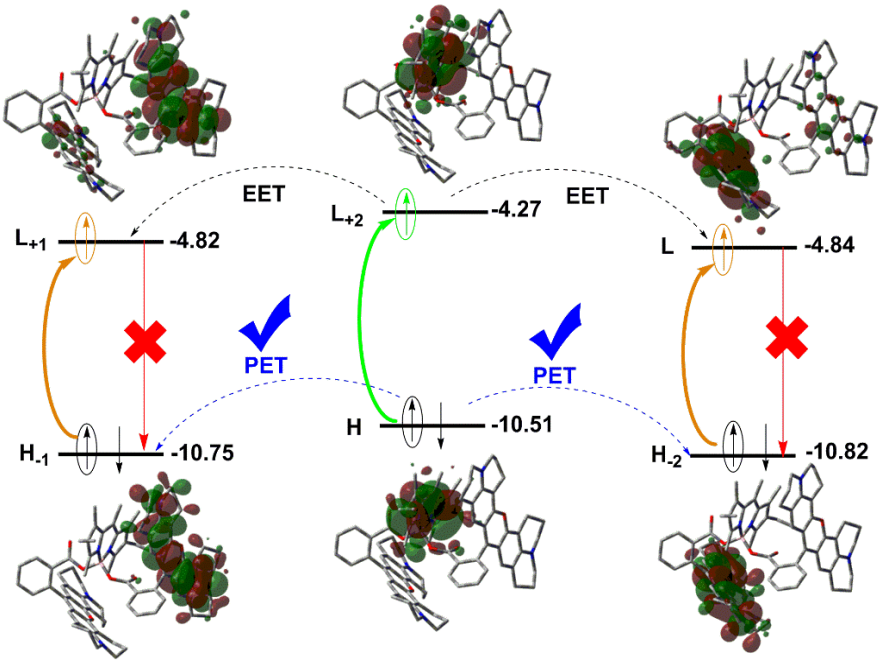

Fig. S12. Computed (wb97xd/6-311g*) localization and energies (eV) of key molecular orbitals in MMA **4f** to illustrate the ongoing BODIPY-to-rhodamine PET, competing with the BODIPY-to-rhodamine EET, upon BODIPY excitation.

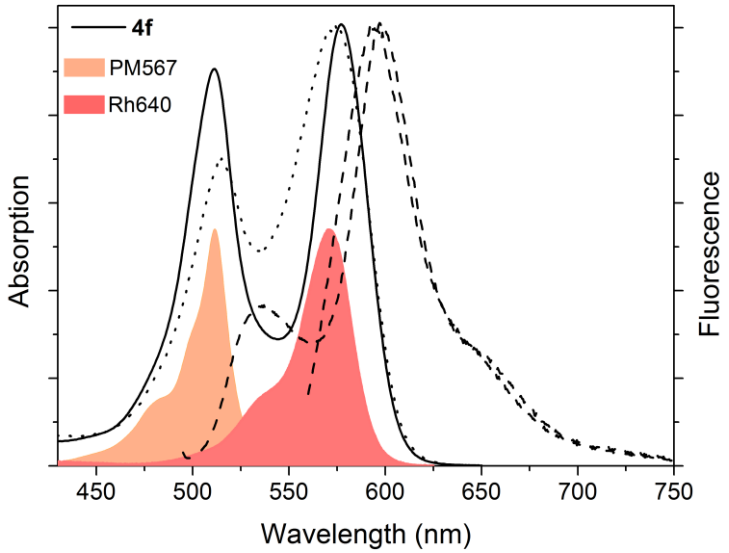

Fig. S13. Normalized UV-vis absorption (bold line), fluorescence spectra (dashed line; after BODIPY- and rhodamine-chromophore selective excitation), and excitation spectra (dotted line; monitored at the rhodamine emission) of the PM567-based MMA **4f** in acetonitrile, as well as UV-vis absorption spectra of the monochromophoric dyes PM567 and rhodamine 640 perchlorate (Rh640) in acetonitrile (filled spectra)

5. References

[1] F. López Arbeloa, J. Bañuelos, V. Martínez, T. Arbeloa and I López Arbeloa, *Int. Rev. Phys. Chem.*, 2005, **24**, 339-374.

[2] M. Liras, M. Iglesias and F. Sánchez, *Macromolecules*, 2016, **49**, 1666-1673.

[3] S. Guo, H. Zhang, L. Huang, Z. Guo, G. Xiong and J. Zhao, *Chem. Commun.*, 2013, **49**, 8689-8691.